Characterization of Flow in Laboratory and Rock Fractures Using an In-Well Point Velocity Probe

By

Bryan R. Heyer
B.S., University of the Sciences in Philadelphia, 2018

Submitted to the graduate degree program in Geology and the Graduate Faculty of the University of Kansas in partial fulfillment of the requirements for the degree of Master of Science.

Chair: J.F. Devlin

Gaisheng Liu

George Tsoflias

Date Defended: 16 March 2021

The thesis committee for Bryan R. Heyer certifies that this is the approved version of the following thesis:

Characterization of Flow in Laboratory and Rock Fractures Using an In-Well Point Velocity Probe

Chairperson: J.F. Devlin

Date Approved: 16 March 2021

Abstract

The In-Well Point Velocity Probe (IWPVP) is a tool deployed in the screened interval of a well that utilizes an internal small-scale tracer test to directly measure groundwater velocity on the centimeter scale. The ability of the tool to function within a well-developed screened portion of a porous media well led to the hypothesis that the IWPVP could also be utilized in fractured rock. A fracture flow apparatus (FFA) was built to conduct preliminary work in the laboratory and allow design adaptations to ensure the IWPVP would properly measure flow magnitude and direction. Calibration factors dependent on well diameter and aperture size were determined experimentally and agreed well with predictions based on a flux balance. Additionally, the IWPVP could identify flow direction accurately to within about ± 15° under idealized laboratory testing conditions. Following successful laboratory work, field testing of adapted IWPVPs (3" and 6" diameter) was carried out at a contaminated fractured rock aquifer at Edwards Air Force Base in California. The IWPVPs were able to identify zones of both relatively low and high flow, in agreement with a variety of other technologies used on site, including passive flux meters, oxidation-reduction sensors, and FLUTe liners. Fluxes internal to the probes were observed to range between 300 – 5,300 cm/d. Additional data on discrete fractures from acoustic borehole televiewers allowed determination of calibration factors from which water fluxes in the fractures were estimated to range from 370 cm/d – 2,239 cm/d. Also, flow directions determined by the IWPVP compared favorably to expected regional flow direction and showed the drastic impact a rain event had on flow directions in the fractures. Overall, this work has supported the IWPVP's use in fractured rock in addition to porous media. With minor adaptations, the probe was able to successfully characterize fracture flow on the centimeter-scale, in near real-time, and at a low fabrication cost.

Acknowledgments

This work was made possible through funding provided by GSI Environmental Inc., the Department of Geology at the University of Kansas, the University Consortium for Field Focused Groundwater Research, University of Guelph, and BP Remediation Management Services Company.

I would like to acknowledge Andrew Kirkman, Beth Parker, Allison Cormican, and Matt Jones for helpful discussions and contributions to this work throughout. Allen Hase and Mark Stockham of the Physics Workshop at the University of Kansas are also acknowledged for their ingenious design ideas and assistance with fabrication of all sorts. I would also like to thank my committee members Dr. Gaisheng Liu and Dr. George Tsoflias for their continued input and review of my work here at KU.

Finally and most importantly, I'd like to acknowledge and thank my advisor, Dr. Rick Devlin, and labmate (but essentially second advisor), Trevor Osorno. From countless hours in the field, lab, office, and via Zoom, you both taught me so much about the field of hydrogeology and even more about the suite of Point Velocity Probes. I have gained so much knowledge on a wide variety of topics from Rick's wealth of information and felt confident working on this research with guidance from Trevor from the very start. I feel any of my success should be attributed to your extraordinary mentorship, which I appreciate greatly.

Table of Contents

List of Figures

List of Tables

1.0 – Introduction

1.1 Groundwater Velocity Characterization

Detailed characterization of contaminated sites is necessary for the optimization of risk analysis, monitoring techniques, and remediation strategies. Since advection is commonly the dominant factor in the transport of contaminants, determining groundwater velocity is a basic goal of characterization efforts (Mackay *et al.*, 1985; Devlin, 2020). The extent of a contaminant's spread is determined to a large extent by groundwater velocity but can be complicated by a variety of factors associated with the aquifer's small-scale or large-scale heterogeneity, resulting in irregular spatial distribution of contaminant mass developing, which may also change in time (Mackay *et al.*, 1985; Guilbeault et al., 2005). As a result, to fully understand contaminant mass flux and discharge, centimeter-scale measurements made at multiple locations of both groundwater velocity and contaminant concentration can be of great value.

Typically, Darcy's Law is utilized to estimate groundwater seepage velocity. However, the parameters necessary for this approach include hydraulic conductivity, effective porosity, and hydraulic gradient, all of which are well understood to contribute notable uncertainties to velocity estimates (Butler *et al.*, 2007; Devlin & McElwee, 2007; Ricciardi *et al.*, 2009; Alexander *et al.*, 2011; Post & von Asmuth, 2013). To avoid these sources of uncertainty, the velocity of groundwater can be measured directly. In most cases, the direct measurement of water flow involves the addition of heat or chemical tracers and, possibly, the use of specialized flux meters or flowmeters (Slichter, 1905; Kerfood and Massard, 1985; Momii *et al.*, 1993; Kearl, 1997; Annable *et al.*, 2005). Larger-scale natural gradient tracer tests can also be useful

but are material and labor intensive, so smaller scale tests using tracers are attractive alternatives in most cases (Kearl, 1997; Bayless *et al.*, 2011).

A tool that directly measures groundwater velocity (through the use of tracers) at the centimeter scale, while in direct contact with the aquifer, is the Point Velocity Probe (PVP) (Labaky *et al.*, 2007). The probe functions by conducting a small-scale tracer test on its outer surface. Typically, a salt tracer is used to generate conductivity signals that register breakthrough curves (BTCs) on the probe detectors. These BTCs can be used to obtain velocity estimates by fitting them with a one-dimensional advection-dispersion equation solution or analyzing them by the method of moments. The benefits of PVPs include their low fabrication cost and ability to conduct time series measurements. In addition, a vertical array of PVPs can be assembled and installed to collect vertically distributed data within an aquifer. PVPs have been demonstrated in the field (Labaky *et al.*, 2009). However, these instruments are designed for deployment in non-cohesive sediments that collapse against the hardware in the borehole. This environment-specific limitation, together with the requirement for a dedicated borehole, places limits on the use of the technology.

As an answer to the limitations of PVPs, the In-Well Point Velocity Probe (IWPVP) was developed utilizing the same basic premise of the original PVP, with adaptations made to allow deployment within existing monitoring wells and thereby overcoming the environmental restrictions of the PVP (Osorno *et al.*, 2018). In the case of the IWPVP, the tracer is injected within the body of the probe (as opposed to the surface of the probe), where groundwater flow carries it through a subset of four channels (i.e. one or two channels) intersecting perpendicularly at the center of the probe (Figure 1.1). Each channel contains a detector wire pair for measuring solution conductivity. Breakthrough curve shapes once again provide information about the

A) B)

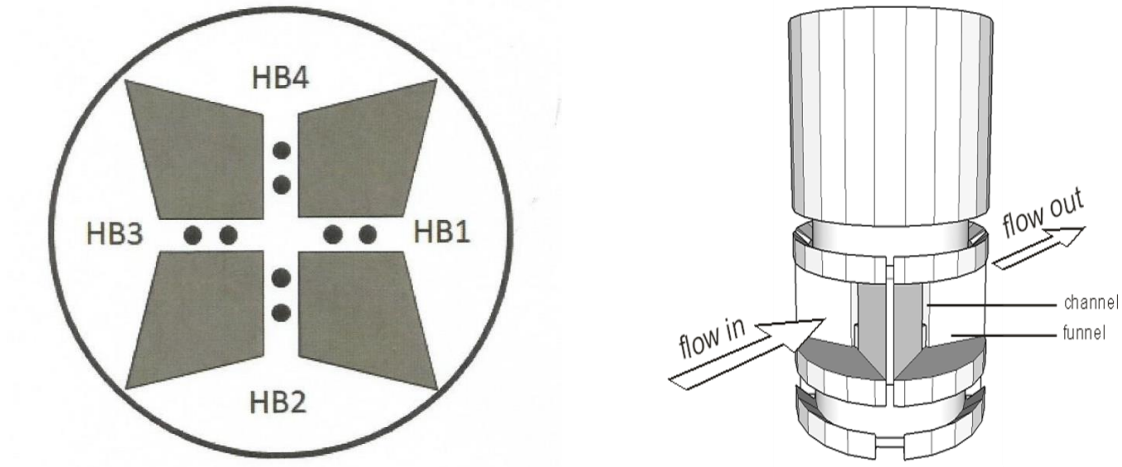

Figure 1.1: A) Plan view of the 4 different channels within the probe body allowing ambient groundwater flow collection and measurement B) An overview of the channel and funnel system that allows passive monitoring of groundwater flow through a well.

velocity of flow, while the specific channel in which BTCs are recorded provide information about the flow direction. The probe body is 3D printed with a diameter corresponding to that of the well in which the measurements will be made. The probe is fitted with flexible brushes between the outer edges of the channels and as collars above and below the channel openings to act as both a simple packer system (minimizing vertical flow and preventing flow around the probe) and as a means to stabilize the probe against the borehole walls. The IWPVP avoids the overhead costs of a dedicated borehole while maintaining many of the benefits of the original PVP, including low cost, direct, and point measurements on the centimeter scale. The IWPVP has been validated for use in porous media settings and has been successfully used in variety of field campaigns, including the characterization of flow at a former refinery site in southern KS (Osorno *et al.*, 2018; Osorno *et al.*, 2020).

1.2 Fractured Media Characterization

Fractured rock is a medium that presents a variety of challenges for characterization and remediation. The parameters of Darcy's Law may be restricted in their applicability to contaminated fractured rock aquifers for reasons of scale, discrete fracture flow, and non-Darcy flow, all of which highlight the advantages of direct measurements of groundwater velocity in this environment (Kohl *et al.*, 1997). Since advection tends to dominate contaminant transport, fractures with low contaminant concentrations but high flow rates are expected to be common and generate a significant contaminant flux (ITRC, 2010). Therefore, if a site underlain by a fractured rock aquifer is not thoroughly characterized, a significant amount of contaminant mass could be easily missed.

Because of the considerations discussed above, it is clear that understanding contaminant transport may require a thorough study of even small-scale features in the geology of an area. As a result, most characterization projects take place in at least two phases: a preliminary effort, focused on obtaining a general assessment, followed by a second, more detailed, investigation. In some cases, a single investigation may suffice, often using a variety of complementary tools (Karasaki *et al.*, 2000). A variety of techniques and tools have been developed or adapted for fractured media-oriented work from porous media methods. As addressed in more detail in Chapter 2, most established techniques are subject to shortcomings associated with drilling and development impacts, assumptions on the amount and size of hydraulically active fractures, artificially induced vertical flow, and time and cost requirements (Novakowski *et al.*, 1985; Novakowski, 1989; Shapiro, 2002; Sterling *et al.*, 2005; Novakowski *et al.*, 2006; Parker *et al.*, 2012; Klammler *et al.*, 2016). More recent technologies developed specifically for use in fractured rock, such as flexible impervious liners (FLUTe™, http://www.flute.com) and fractured rock Passive Flux Meters (FRPFMs) solved some of the shortcomings of the earlier

methods. However, hydraulic characterization conducted with FLUTe liners suffers from decreased resolution with depth and relies on additional tools for flow estimation. The FRPFM requires deployment over several days to weeks to produce time-averaged data and requires laboratory analysis of dye and tracer movement that may not be compatible for certain investigations to assess risk and develop remedial designs (Cherry *et al.*, 2007; Klammer *et al.*, 2016).

In this work, it was hypothesized that the IWPVP could fulfill a role as a tool for fractured rock aquifer characterization due to its low cost and near real-time data acquisition capabilities while avoiding the sources of uncertainty associated with Darcy's Law. Thus, the objectives for this work were to test the viability of the IWPVP in fractured rock and then to adapt its design for optimal performance in fractured media. To accomplish this, Chapter 2 presents a lab-scale model of a single fracture built for initial performance testing of the probe and testing of probe design changes to optimize performance. Chapter 3 presents a field campaign carried out to evaluate the probe's performance in a real-world fracture system. Chapter 4 summarizes the thesis contributions and proposes the next steps for the technology as well as future applications where it may prove to be most useful in conjunction with other methods in use or development.

1.3 References

Alexander, M., Berg, S.J., Illman, W.A., 2011. Field Study of Hydrogeologic Characterization Methods in a Heterogeneous Aquifer. Ground Water 49, 365–382. https://doi.org/10.1111/j.1745-6584.2010.00729.x

Annable, M.D., Hatfield, K., Cho, J., Klammler, H., Parker, B.L., Cherry, J.A., Rao, P.S.C., 2005. Field-scale evaluation of the passive flux meter for simultaneous measurement of groundwater and contaminant fluxes. Environ. Sci. Technol. 39, 7194–7201. https://doi.org/10.1021/es050074g

Bayless, E.R., Mandell, W.A., Ursic, J.R., 2011. Accuracy of Flowmeters Measuring Horizontal Groundwater Flow in an Unconsolidated Aquifer Simulator. Gr. Water Monit. Remediat. 31, 48–62. https://doi.org/10.1111/j.1745-6592.2010.01324.x

Butler, J.J., Dietrich, P., Wittig, V., Christy, T., 2007. Characterizing hydraulic conductivity with the direct-push permeameter. Ground Water 45, 409–419. https://doi.org/10.1111/j.1745-6584.2007.00300.x

Cherry, J.A., Parker, B.L., Keller, C., 2007. A new depth-discrete multilevel monitoring approach for fractured rock. Gr. Water Monit. Remediat. 27, 57–70. https://doi.org/10.1111/j.1745-6592.2007.00137.x

Devlin, J.F., 2020, Groundwater Velocity. The Groundwater Project, Guelph, Ontario, Canada.

Devlin, J.F., McElwee, C.D., 2007. Effects of measurement error on horizontal hydraulic gradient estimates. Ground Water 45, 62–73. https://doi.org/10.1111/j.1745-6584.2006.00249.x

Guilbeault, M.A., Parker, B.L., Cherry, J.A., 2005. Mass and flux distributions from DNAPL zones in sandy aquifers. Ground Water 43, 70–86. https://doi.org/10.1111/j.1745-6584.2005.tb02287.x

ITRC, 2010. Use and Measurement of Mass Flux and Mass Discharge. ITRC Technol. Overv. MASSFLUX-1, 1–154.

Karasaki, K., Freifeld, B., Cohen, A., Grossenbacher, K., Cook, P., Vasco, D., 2000. A multidisciplinary fractured rock characterization study at Raymond field site, Raymond, CA. J. Hydrol. 236, 17–34. https://doi.org/10.1016/S0022-1694(00)00272-9

Kearl, P.M., 1997. Observations of particle movement in a monitoring well using the colloidal borescope. J. Hydrol. 200, 323–344. https://doi.org/10.1016/S0022-1694(97)00026-7

Kerfoot, W.B., Massard, V.A., 1985. Monitoring Well Screen Influences on Direct Flowmeter Measurements. Groundw. Monit. Remediat. 5, 74–77. https://doi.org/10.1111/j.1745-6592.1985.tb00942.x

Kohl, T., Evans, K.F., Hopkirk, R.J., Jung, R., Rybach, L., 1997. Observation and simulation of non-Darcian flow transients in fractured rock. Water Resour. Res. 33, 407–418. https://doi.org/10.1029/96WR03495

Labaky, W., Devlin, J.F., Gillham, R.W., 2007. Probe for measuring groundwater velocity at the centimeter scale. Environ. Sci. Technol. 41, 8453–8458. https://doi.org/10.1021/es0716047

Labaky, W., Devlin, J.F., Gillham, R.W., 2009. Field comparison of the point velocity probe with other groundwater velocity measurement methods. Water Resour. Res. 46, 1–9. https://doi.org/10.1029/2008WR007066

Mackay, D.M., Roberts, P. V., Cherry, J.A., 1985. Transport of organic contaminants in groundwater. Environ. Sci. Technol. 19, 384–392. https://doi.org/10.1021/es00135a001

Momii, K., Jinno, K., Hirano, F., 1993. Laboratory studies on a new laser Doppler Velocimeter System for horizontal groundwater velocity measurements in a borehole. Water Resour. Res. 29, 283–291. https://doi.org/10.1029/92WR01958

Osorno, T.C., Devlin, J.F., Firdous, R., 2018. An In-Well Point Velocity Probe for the rapid determination of groundwater velocity at the centimeter-scale. J. Hydrol. 557, 539–546. https://doi.org/10.1016/j.jhydrol.2017.12.033

Osorno, T.C., Devlin, J.F., Cormican, A., Heyer, B., Jones, M. 2020. Progress Update Report on IWPVP and PVP Data Analysis for Neodesha, KS, November 2019. Addendum to the Biosparge Pilot Test and Amendment Injection Workplan submitted by Sovereign Consulting Inc. to the Kansas Department of Health and Environment, May, 11 pp.

Post, V.E.A., von Asmuth, J.R., 2013. Review: Hydraulic head measurements—new technologies, classic pitfalls. Hydrogeol. J. 21, 737–750. https://doi.org/10.1007/s10040-013-0969-0

Ricciardi, K.L., Pinder, G.F., Karatzas, G.P., 2009. Efficient Groundwater Remediation System Designs with Flow and Concentration Constraints Subject to Uncertainty. J. Water Resour. Plan. Manag. 135, 128–137. https://doi.org/10.1061/(asce)0733-9496(2009)135:2(128)

Slichter, C.S., 1905. Field measurements of the rate of movement of underground waters, U. S. Geological Survey Water-Supply and Irrigation Paper 140. https://doi.org/10.3133/wsp140

2.0 – Laboratory testing of real-time flux measurements in fractured media

2.1 – Abstract

The In-Well Point Velocity Probe (IWPVP) was originally developed for use in screened porous media wells. The tool can characterize small-scale aquifer heterogeneity from wells that have been carefully developed to ensure an open screen and good hydraulic connection with the surrounding aquifer. This capability led to the hypothesis that the IWPVP could be adapted to characterize flow in fractured media, which features small scale openings (i.e. fractures) that resemble screen slots. To test this hypothesis, a lab-scale fracture flow apparatus (FFA) was fabricated. The FFA consisted of two parallel acrylic plates that could be separated by a fixed distance, simulating a fracture with a known aperture. Two lengths of PVC well casing served as a cylindrical access port and were centrally placed in the plates. This mock-well left the interface with the fracture open – analogous to a fracture intersecting an uncased borehole. The probe was calibrated experimentally by relating known fluxes through the FFA with those measured inside the IWPVP. The ratio of these fluxes was found to be predictable for two aperture sizes (500 μm and 1,290 μm), based on a flux balance and the Cubic Law. Additionally, the ability of the probe to discern flow direction in a fracture was tested and found to be accurate within about ± 15° under the conditions of the laboratory testing. The results suggest that an IWPVP could be reliably used in fractured media to directly measure horizontal flux and flow direction in a single fracture without reference to Darcy's Law.

2.2 – Introduction

Knowledge of the flow in discrete fractures is fundamental to assessing risk in contaminated fractured aquifers. For example, a low-flow fracture with a high concentration of a contaminant may generate a negligible contaminant flux compared to another fracture with high-

flow rates but a lower concentration of the contaminant (ITRC, 2010). Traditional techniques for characterizing flow in fractured media have borrowed from porous media investigations, including the uses of pumping tests, tracer tests, slug tests, and forced-gradient tests (Gernand and Heidtman, 1997). Because the storativity of some fractured rock types can be small relative to porous media, a result of flow constrained to small, high-permeability pathways through a comparatively low-porosity matrix, pumping tests are very strongly influenced by drilling artifacts, wellbore storage, and skin effects (Novakowski, 1989). To better handle the low-storativity values, pulse interference tests were developed, however they are also subject to well skin effects, in addition to requiring several hours to obtain minimum datasets (Johnson *et al.,* 1966; Novakowski, 1990). Researchers have also noted that tracer tests in fractured rock with a network of intersecting fractures are quite difficult to interpret and nonunique model solutions are common (Tester *et al.,* 1982; Landstrom *et al.,* 1983). A single fracture can be evaluated via tracer injection, but it requires detailed prior knowledge of the fracture, including its hydraulic connection between the pumping and extraction boreholes. Precise pumping rates are also essential to deal with the small water volumes and high velocities expected through a fracture. The estimation of hydraulic apertures is imprecise and usually depends on assumptions that all identified openings are hydraulically active and the same size as well as induced flow conditions which can also bias estimates high (Novakowski *et al.,* 1985; Parker *et al.,* 2012).

Recent advances in fractured rock hydrogeology have in many cases been achieved using single instrumented boreholes and screened wells, e.g. flux/flow meters, velocimeters, borescopes, packer-enclosed techniques. Unfortunately, these approaches tend to introduce biases because they – or the consequences of their use – produce artificial vertical connections between otherwise isolated, discrete fractures (Shapiro, 2002; Sterling *et al.,* 2005; Novakowski

et al., 2006). As a result, the borehole can serve as a relatively large artificial reservoir in the aquifer. Historically, predictions based on pumping and injection tests in open boreholes and wells have led to underestimations of solute spreading (Berkowitz, 2002).

Over the past two decades, specialized technologies have been introduced that are geared towards quantifying the flow in individual fractures. These include passive flux meters, geophysical techniques, heat pulse flow meters, colloidal borescopes, and acoustic doppler velocimeters (Wilson *et al*., 2001; Hatfield *et al*., 2004; Tsoflias *et al*., 2004; Annable *et al*., 2005). However, the performances of these in-well devices has been limited by phenomena such as artificial vertical flow in the borehole and borehole-induced horizontal flow direction changes that are not representative of natural conditions (Shapiro, 2002; Novakowski *et al*., 2006; Klammler *et al*., 2016). The isolation of small portions of a borehole with packers can sometimes improve the quality of measurements. However, tests such as packer-enclosed point dilution tests have been reported to exhibit concerning levels of variability and poor proportionality between aperture size and velocity (Novakowski *et al.*, 2006). This establishes that the use of packers is not an assured method of obtaining flow measurements with high levels of confidence.

In response to the ongoing need for new methods to quantify fracture flow, new tools are being developed and tested in fractured media. Flexible impervious liners (FLUTe™, http://www.flute.com) line boreholes and reestablish the isolation of fractures that intersect the borehole. Depth-specific estimates of hydraulic transmissivity can be obtained by recording pressure head as the liner is deployed downward in the borehole. However, resolution declines as the liner approaches the bottom of the borehole since water has fewer pathways to enter the formation at these depths, and the pressure in the borehole increases rapidly while liner deployment speed decreases. Once the liner is in place, estimates of flow may be obtained using

heat-sensing instruments positioned between the liner and the formation (Cherry *et al.*, 2007). The general approach of using temperature to infer flow has also been described using distributed temperature sensing cables installed in the borehole filled with grout (Maldaner *et al,* 2019).

Another promising recent development in this field is a passive flux meter designed explicitly for fractured media by measuring time-averaged water and contaminant fluxes and fracture network properties through consolidated rock (Klammler *et al.*, 2016). The device consists of an inflatable core with a thin permeable layer of elastic fabric mesh that contains dye. The leaching of dye from the mesh reveals patterns that provide insight into the location and extent of the fracturing. The area of the leached zone can, in principle, be used to estimate the cumulative magnitude of groundwater flow and contaminant mass flux in the relevant fracture(s). Such fluxes were estimated to within about 25% of expected values in controlled laboratory tests. The time-averaged nature of the measurements is advantageous for some assessments of risk, but the method is poorly suited to record short-term surges of water or contaminants, which may be relevant for other risk considerations and remedial designs. Furthermore, the time to acquire a measurement may be several days to several weeks, ruling out the method where quick responses are desired (Klammler *et al.*, 2016).

A relatively recent tool that may be adaptable to fractured systems and that yields test results in near real-time is the In-Well Point Velocity Probe (IWPVP). The IWPVP was developed as a tool for deployment in standard monitoring wells to determine groundwater velocity (Osorno *et al.*, 2018). The IWPVP operates by conducting a miniature tracer test within the body of the probe, revealing the movement of groundwater in the well and, ideally, the surrounding aquifer (Figure 2.1). A chief advantage of the IWPVP is its ability to circumvent the

use of Darcy's Law, therefore, eliminating uncertainties associated to hydraulic conductivity (*K*), porosity, and gradient (Butler *et al.*, 2007; Devlin & McElwee, 2007; Ricciardi *et al.*, 2009; Alexander *et al.*, 2011; Post & von Asmuth, 2013). Additionally, due to the discrete sampling interval of the IWPVP (~ 2 – 3 cm) localized small-scale variations of flow in aquifers can be characterized, which have been shown to have significant impacts on transport processes (Feenstra *et al.*, 1984; Sudicky, 1986; Bianchi *et al.*, 2011; Schillig *et al.*, 2016). A further advantage of the IWPVP is the magnification of flow within the device creating extremely short duration measurements (typically less than 20 minutes). The short measurement durations allow for many tests to be conducted across a site in a period of a few days. Rapid site-wide sampling or system-based testing provides the ability to verify conceptual models with field-based flow data. This novel, portable, and reusable device has been demonstrated to rapidly determine depth-specific groundwater fluxes both in laboratory and field experiments (Osorno *et al.*, 2018; Heyer *et al.*, 2019; Osorno *et al.*, 2020).

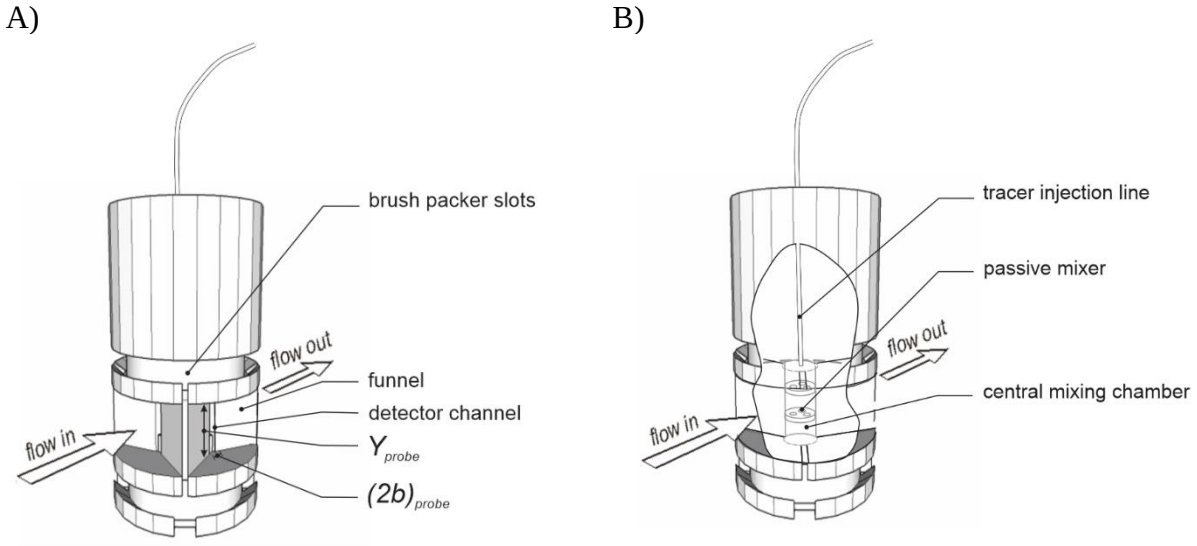

Figure 2.1: Schematic of the IWPVP. A) external features, highlighting channel and funnel system, location of packer brush insertion slots, and related cross-sectional area. B) internal features as related to conducting internal miniature tracer tests.

The success of the original IWPVP's performance in quantifying flow over centimeter-scale sections of wells suggested the tool might be used with similar success in fractured media, which also exhibits pronounced small-scale variations in flow intersecting a borehole (Cacas *et al.*, 1990; Berkowitz, 2002). As such, the IWPVP could serve a complimentary role in fractured rock hydrogeological investigations when applied with other novel and conventional systems. Thus, the overall goals of this work were to test the hypothesis that the IWPVP could be used to characterize discrete fractures and modify the probe design as required to optimize that function.

2.3 – Materials and Methods

2.3.1 – Fracture Flow Apparatus (FFA) Design

In order to carry out preliminary testing of the IWPVP in a fractured media setting, a laboratory scale model of a fracture, the fracture flow apparatus (FFA), was fabricated (Figure 2.2). The IWPVP was designed specifically to measure horizontal flow through vertical boreholes, so the physical model incorporated a single, horizontal fracture. The FFA design was similar to that reported by Klammler *et al.* (2016) and consisted of two 40 x 63 cm parallel acrylic sheets positioned at specified distances apart (500 or 1,290 µm) to emulate single fractures with different apertures. Flow was controlled by a peristaltic pump and introduced to the system via an inlet port located in a channel in the bottom acrylic sheet. The flow was permitted to leave the FFA at the opposite end of the system via an outlet channel and port also in the lower plate. The channels served as constant head boundaries at each end of the fracture. Ten smaller ports were added to the bottom plate for the purposes of conducting dye tracer visualization tests (red box in Figure 2.2). A hole was cut into each plate to accommodate two short lengths of 5 cm diameter PVC casing, which mimicked a well casing to house the IWPVP. The casing lengths terminated at the inside faces of each plate, so the fracture transitioned

seamlessly into the mock-well. In this work, the FFA utilized set screws to establish and maintain as consistent an aperture size as possible across the plates. Additionally, wires with gauges equal to the desired aperture size were placed along the edges of the plates to provide additional support and uniformity to the aperture.

A)

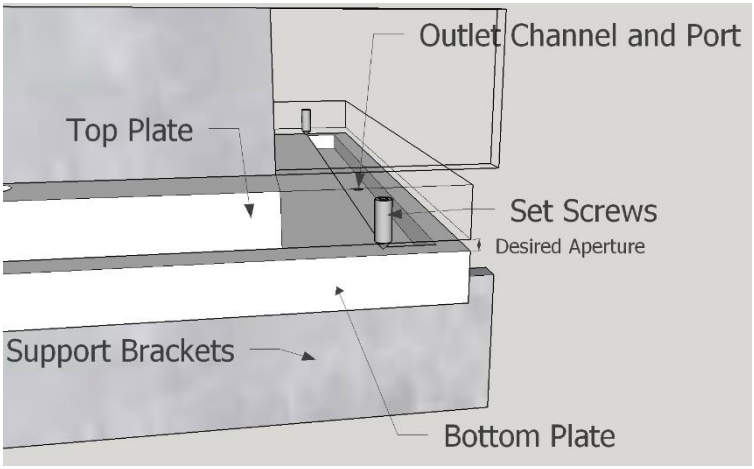

B)

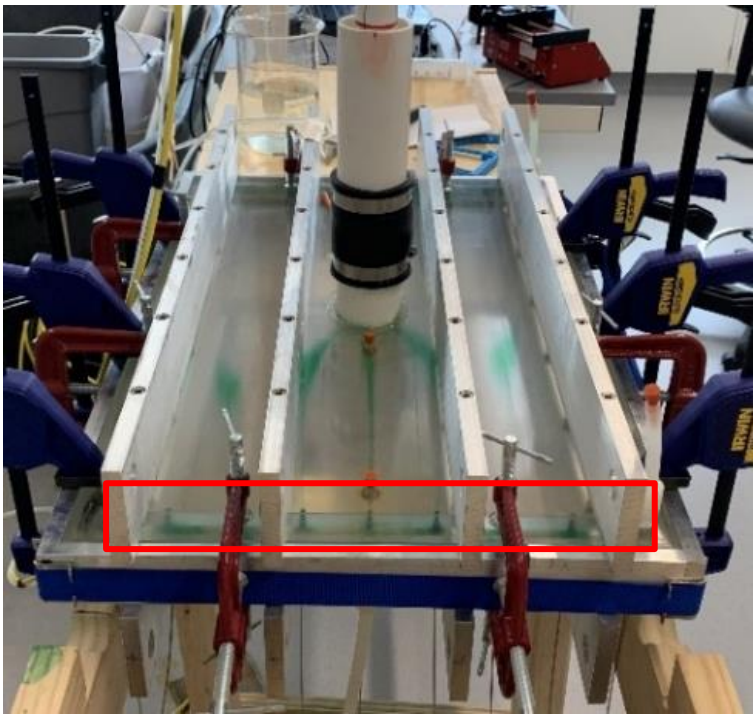

Figure 2.2: A) 3D sketch of important aspects of the FFA for maintaining a constant aperture and flow throughout the system. B) The fully assembled and operational FFA (40 cm wide x 63 cm long) with a dye trace experiment in progress. The red box highlights tracer injection points, as well as constant head channel.

2.3.2 – Modeling

Numerical modeling of flow in the laboratory fracture apparatus was carried out for the dual purposes of designing the apparatus and later data interpretation. Water flux in the fracture was calculated from the cubic law equation (Zimmerman & Bodvarsson, 1996),

$$Q_f = q_f A = K_f A \nabla h = \frac{(2b)_f{}^3 W \rho g}{12\mu} \nabla h \quad (1)$$

where, Q_f is discharge (LT^{-3}), q_f is flux (LT^{-1}), A is the cross-sectional area for flow (L^2), $(2b)_f$ is the fracture aperture (L), K_f is a fracture hydraulic conductivity (LT^{-1}), W is the fracture width (L), ρ is water density (ML^{-3}), g is acceleration due to gravity (LT^{-2}), μ is the coefficient of dynamic viscosity of water ($ML^{-1}T^{-1}$), and h is the hydraulic head (L).

Two-dimensional flow modeling was performed iteratively using Excel with a convergence criterion of 0.0001. Steady state flow was simulated in the fracture with a finite difference solution to the two-dimensional flow equation,

$$K_{fx} \frac{\partial^2 h}{\partial x^2} + K_{fy} \frac{\partial^2 h}{\partial y^2} = 0 \quad (2)$$

where x and y are cartesian coordinate values (L) and K_{fx} , K_{fy} are direction-specific, effective fracture hydraulic conductivities (LT^{-1}). Constant flux boundaries were used along the inflow and outflow sides of the model, and no-flow boundaries were used along the sides parallel to flow. The model domain size was set to the same dimensions as the FFA (40 cm x 63 cm) on a 100 x 66 grid discretization with equal Dx and Dy values. The entire apparatus was modelled to ensure that the boundary conditions had no impact on flow near the well. A series of simulations

were run with various well diameters to establish that flow results with a 5 cm well were not impacted by the boundaries.

The acrylic plates appeared smooth and flat to the naked eye, but at the micron scale, the manufacturing process generated some variation. To assess the bias caused by these variations, several numerical simulations of the FFA were performed with random deviations from uniformity in the aperture value, up to 10% to represent the natural variation in thickness from manufacturing. The ± 10% variation was chosen based on measurements of plate flatness made during the FFA fabrication and represents a maximum in the observed deviations from flatness.

2.3.3 – Probe Calibration

The IWPVP was first deployed in the mock-well with an orientation that provided flow with a straight path through the probe (note that later testing, geared at evaluating flow direction assessment, involved the probe rotated in the well, see *section 2.4*). IWPVP tests were initially performed with a saline tracer introduced at the top of the central mixing chamber that was allowed to descend via density-driven flow. As this occurs, the groundwater flow through the probe carries the tracer into the detector channel(s) and over the detector wires.

Among the tests reported here, some were conducted with 0.5 g/L NaCl tracer solutions and others with deionized water. Tracer injections were accomplished using a syringe pump (NE-4000 Programmable Syringe Pump – New Era Pump Systems, Inc.). Tracer volume was restricted to between 0.01 and 0.1 mL, which means the average injection volume is less than 10% of the internal probe mixing channel volume. These volumes were selected because in prior laboratory testing, measured flux inside the probe began to show a positive bias when the injections exceeded 0.1 mL.

The IWPVP was connected to a CR1000 datalogger (Campbell Scientific) through a half-bridge circuit using 2.2 kilo-ohm resistors (details given in Devlin *et al.,* 2009). The datalogger was programmed to record the resistivity from the detectors at 1 second intervals. Following the tests, the data were downloaded using Campbell Scientific LoggerNet v.4.5 software, and the breakthrough signals interpreted with VelprobePE 3.1 beta d (Schillig, 2012; Schillig and Devlin, 2018).

2.3.4 – Flow Direction Determination

In principle, the IWPVP will indicate flow direction to at least ± 45° due to the quadrant design of the flow channels that controls where water can exit the probe. However, better estimates of flow direction can be obtained by analyzing the relative amounts of flow in the exiting channels, as described by Osorno *et al.* (2018) (Equation 3). The degree to which a direction measurement in the probe is representative of the flow direction in the aquifer depends on the condition of the well screen, or filter pack if present. If two BTCs with signals of similar strength are observed in neighboring channels, the overall flow direction is interpreted as a mass-weighted vector addition of the contributions from each channel,

$$\theta_{app} = tan^{-1} \frac{(v_1)W_1}{(v_2)W_2} \quad (3)$$

where θ_{app} is the apparent angle of flow relative to probe channel v_2, $v_{1,2}$ are the estimated velocities through each channel, and $W_{1,2}$ are the mass fraction weights of the tracer (assumed equal to areas under the BTCs) in each channel.

In order to test the capability of the IWPVP to determine flow direction in the FFA, the probe was first emplaced with inlet and outlet channels aligned with the flow direction. In a

subsequent series of tests, the probe was removed from the well, rotated approximately 10° and reinstalled. This procedure was repeated until a total rotation of 90° was achieved. The splitting of tracer between channels was assessed with Equation 3 and compared to the known angles between the channels and the actual flow direction. All tests were performed in either triplicate or quadruplicate.

2.4 – Results and Discussion

2.4.1 – Assessing Fracture Flow Apparatus (FFA) Hydraulics

The Cubic Law equation was utilized in modelling efforts to assess the flow of water through the FFA. Equation 1 shows the relationship between the specific discharge, q_f, effective fracture hydraulic conductivity, K_f, and the fracture aperture, (2b). Rearranging and combining terms in Equation 1 results in Equation 4,

$$q_f = \frac{Q}{(2b)_f W} \tag{4}$$

where, the denominator term $(2b)_f W$ represents the cross-sectional area to flow, A, in Equation 1, and W is the width of the FFA apparatus (40 cm) (L). This calculated estimate of q_f was compared to the experimentally derived value obtained by observing the movement of a colored dye through the apparatus. For a fracture aperture of 500 µm and a pumping rate of 5.34 mL/min, Equation 4 predicts a q_f of 2.56 cm/min. Experimentally, under these conditions, the dye movement proceeded at 2.67 cm/min, indicating the FFA was performing as designed (Figure 2.3).

As a further check on the FFA hydraulics, the width of the well capture zone (Y_c) observed in the dye test was compared to the capture width predicted numerically (Figure 2.3). In both cases, the value of Y_c was found to be within 9 ± 1 cm. When the variability in plate

thickness was taken into account in the numerical modeling (by varying $(2b)_f$ randomly on a node by node basis and using Equation 1 to obtain the corresponding values of K_f), in no cases did the simulations indicate any notable change in the average seepage velocity (~6 cm/min ± 2% standard error) or capture width. These assessments provide corroborating evidence that the apparatus could achieve reliable and predictable baseline velocity data for evaluating the IWPVP over the range of apertures studied.

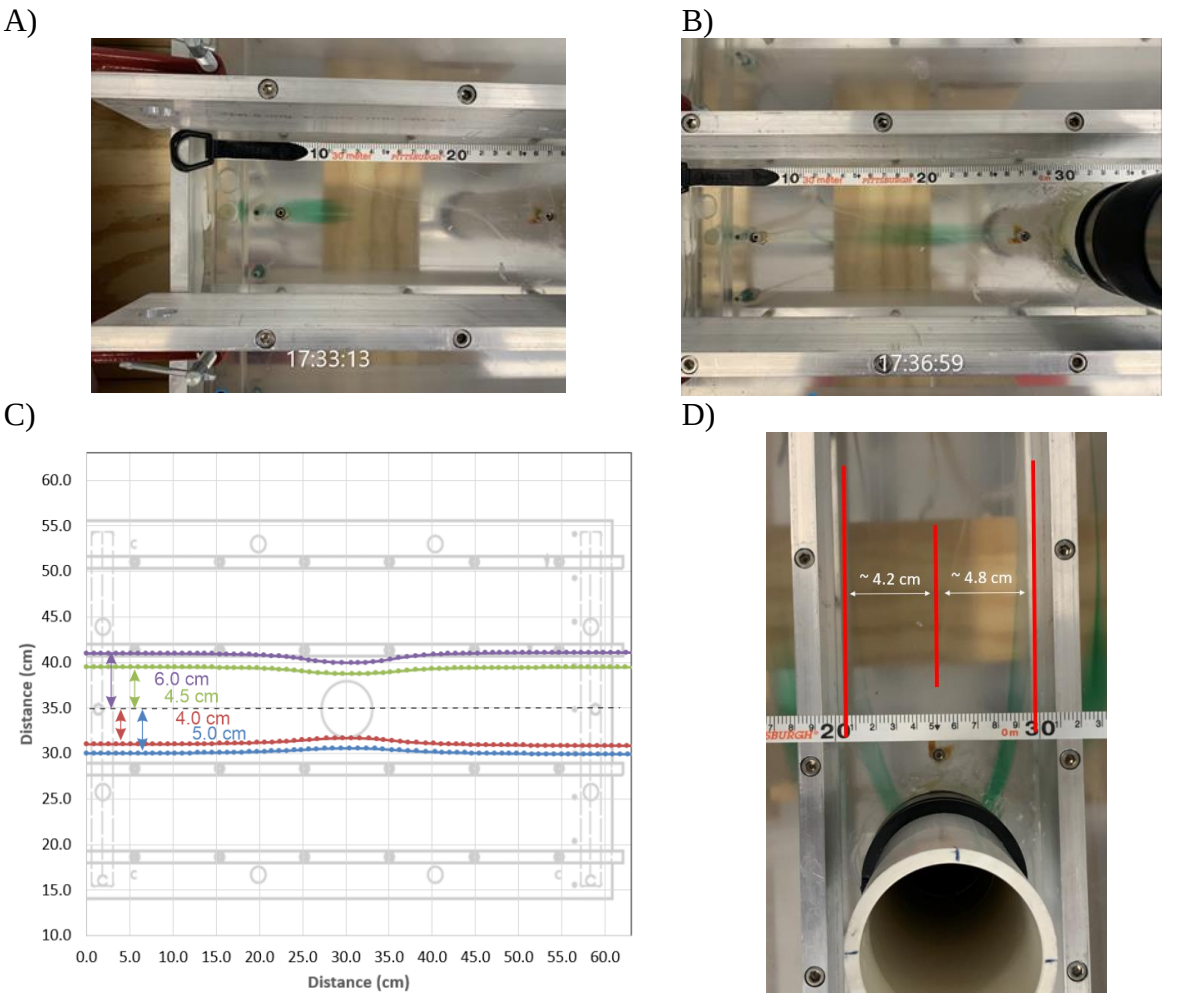

Figure 2.3: Injected dye tracer test of linear velocity and comparison of predicted and experimental capture zones of the well intersecting the laboratory model of a single fracture. A) Center of mass of dye crossing 10 cm distance at 17:33:13 B) Center of mass of dye crossing 20 cm distance at 17:36:50 C) Particle tracks about 4 to 5 cm on either side of the centerline converge on the well. D) Tracer dye released about 4.2 cm from the centerline marks the outer limit of the capture zone experimentally.

2.4.2 – IWPVP Adaptation to Fractured Settings

The IWPVP testing was completed in two phases. In the first phase, the probe design adopted was taken directly from earlier porous media applications and applied to the FFA as a preliminary test of viability. In the second phase, the design was modified to improve performance in the fracture setting. Phase 1 testing established that the IWPVP could record readily identifiable signals (i.e., clear breakthrough curves, BTCs) in a fracture environment, but in some cases the BTCs exhibited a bimodal quality (Figure 2.4A). It was hypothesized that the peak pairs represented two distinct zones of flushing within the IWPVP mixing chamber. The first zone was thought to exist approximately in the plane of the fracture. The second zone occupied the remaining volume in the mixing chamber, above and below the plane of the fracture. It was reasoned that if this hypothesis described the phenomena generally correctly, the first peak would reflect the flow in the fracture best, while the second would be more susceptible to variable mixing efficiency in the probe and perturbations related to the relative probe position and orientation intersecting the fracture.

The two-zone conceptual model of mixing in the probe suggests that all aspects of the detector signals should be sensitive to the overall flushing rate, i.e., the test pumping rates. Moreover, because the two peaks observed in the signals would be expected to flush with different efficiencies, the bimodal character of the BTCs should change with pumping rate. Therefore, to test the above hypothesis, a series of variable flow rate tests were conducted. As expected, these tests yielded BTCs that were dependent on the flow rate. At flow rates less than 1.8 mL/min, tests were characterized by unimodal BTCs, presumably because flow through the probe was slow enough for the two zones to effectively mix (Figure 2.4B). At flow rates greater than about 9 mL/min, the BTCs were also characterized by single peaks (Figure 2.4C). Here, the

higher flow rates are thought to have created turbulent mixing in the probe that again led to well-blended tracer mass on and off the fracture plane. At intermediate flow rates, the bimodal BTCs could be reproducibly generated. Tests in this intermediate range produced BTCs that behaved as expected: the first BTC was a linear function of the flow rate in the fracture over a range of specific discharges from 700 cm/d to 8,000 cm/d. The second BTC exhibited more variability and was only reliably linear up to 3,500 cm/d through the fracture.

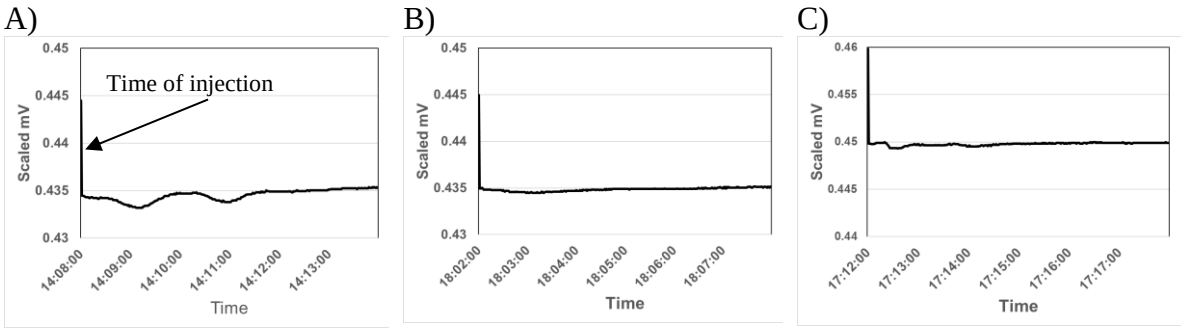

Figure 2.4: A) Bimodal breakthrough curves resulting from injection of salt tracer, causing downward-facing "peaks" B) A unimodal, small breakthrough curve resulting from low flow rates C) a single, quick breakthrough curve resulting from higher flow rates

In phase 2 testing, the probe was modified to minimize the signal split, and the modifications were evaluated. The first modification released the tracer in a more controlled fashion in the center of the IWPVP measurement channel. Preliminary tests were performed using saline tracer to ensure that results were acceptable, but subsequent detailed testing reported below was conducted with a deionized water tracer. A needle was positioned so that it terminated at the center of the central mixing chamber (Figure 2.5). This alteration better localized the initial tracer introduction in the chamber and increased the single BTC signal strength over the entire range of velocities tested (700 cm/d to 8,000 cm/d) (Figure 2.6). In addition, this modification effectively eliminated the bimodal character of BTCs at all flow rates tested.

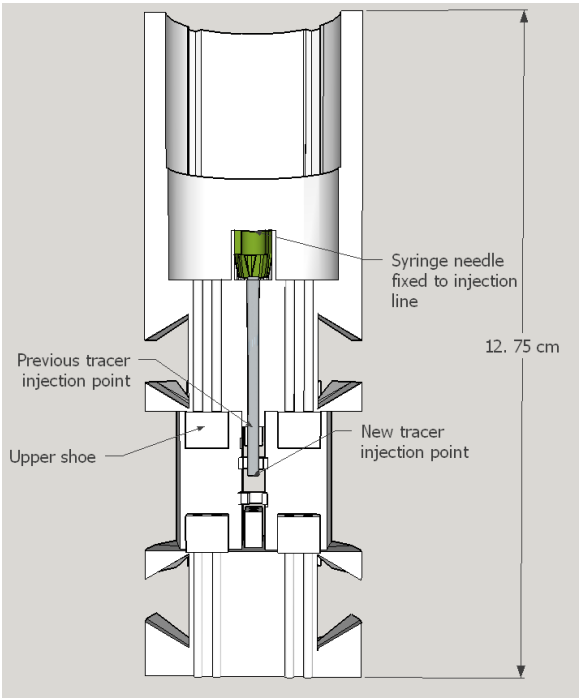

Figure 2.5: Cross section of the updated probe design highlighting the more precise injection system centered within the probe channels

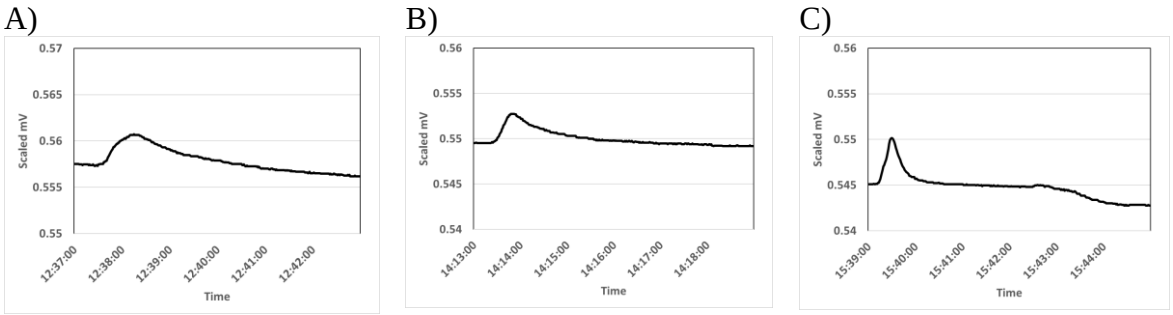

Figure 2.6: Deionized water tracer breakthrough curves produced by the updated probe at a variety of flux velocities: A) 2,000 cm/d B) 4,750 cm/d C) 6,250 cm/d

An additional modification to the IWPVP design was made to accommodate the use of either deionized water or saline solutions as tracers. Insulating ‘shoes’ were added to the top of the channels mimicking those that were part of the original design for the floor of the probe (Figure 2.5). These features ensured that density- (or buoyancy-) driven flow that exited the

probe on the floor or ceiling did not cause a signal on the detectors (Osorno *et al.*, 2018). Only tracer carried through the central portions of the channels due to ambient groundwater flow elicited detector responses; density driven flow or buoyancy driven flow were not sensed.

2.4.3 – Calibration

A calibration factor was calculated to convert the measured fluxes in the IWPVP to seepage velocities in the surrounding fracture, as described by Osorno *et al.* (2018). Note that the probe measures a specific discharge, q_{probe} in this case, because porosity in the probe is one (i.e., $q_{probe} = v/n_{probe}$). In the case of a single fracture, also with a porosity of 1, flux measured in the probe can be converted to discharge in the probe (Q) ($Q=(q_f A_p$ where A_p is the cross-sectional area in a probe channel, and given by $Y_{probe} \times 2b_{probe} = 27\ mm \times 4.5\ mm$) which must be equal to flow in the portion of the fracture captured by the well containing the probe, i.e., the capture zone. The Cubic Law (Equation 1) can then be used to estimate the water flux in the fracture, q_f,

$$q_f = \frac{Q}{(2b)_f Y_c} \tag{5}$$

where, Y_c is the capture zone width defined above. Equation 5 can be developed both for the fracture and for the detector channels in the probe (Figure 2.1). Since Q is common to the probe and the fracture capture zone, it follows that,

$$Q = q_f (2b)_f Y_c \tag{6}$$

$$Q = q_{probe} (2b)_{probe} Y_{probe} \tag{7}$$

$$\frac{q_{probe}}{q_f} = \frac{(2b)_f Y_c}{(2b)_{probe} Y_{probe}} \tag{8}$$

Equation 8 shows that the ratio of fluxes (i.e., the calibration factor) in the probe and that the fracture is a function of the fracture aperture. If the capture width is known in advance (recall $(2b)_{probe}$, Y_{probe} are known constants determined in the probe design), this relationship reduces to a simple linear one. However, the Cubic Law (Equation 1) indicates that the capture zone width varies inversely with the cube of fracture aperture, so if Y_c is uncertain, Equations 5 and 8 could propagate considerable error to the estimation of q_f. This possibility was evaluated experimentally and with numerical modeling.

The fluxes measured with the probe were plotted against the predicted fluxes from Equation 5 (Figure 2.8). The calibration line was found to be linear, but lower in slope than the previously observed lines for porous media applications. This difference is easily understood on the basis of Equation 8 and its porous medium equivalent (see Equations 10 and 11). For porous media, Equation 8 becomes

$$\frac{Q_{probe}}{Q_{capture}} = 1 = \frac{q_{probe} Y_{probe} (2b)_{probe}}{q_{pm} Y_c z_{pm}} \tag{9}$$

$$\frac{q_{probe}}{q_{pm}} = \frac{Y_c z_{pm}}{(2b)_{probe} Y_{probe}} \tag{10}$$

where z_{pm} and Y_c are the vertical and horizontal extents of the capture zone of the well, respectively, and $Q_{capture}$ is the flow in the formation captured by the well (Figure 2.7).

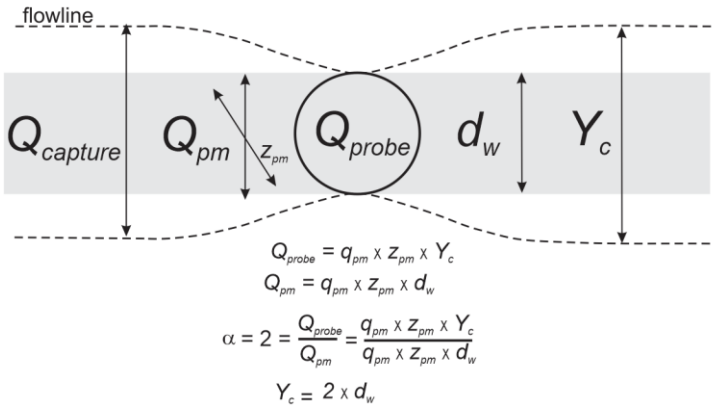

Figure 2.7: Simplified derivation of a well capture width, Y_c, as a function of well diameter, d_w, based on the convergence factor value $\alpha = Q_{probe}/Q_{pm}$ calculated with Equation 11. With a convergence factor of 2 from Equation 12, the capture zone is twice the diameter of the well.

According to Ogilvi *et al.*, (1958) as reported by Halevy *et al.* (1967), the capture width for a well of diameter 5.1 cm, with no filter pack, and a screen with permeability much greater than the surrounding formation, the follow equation applies:

$$\alpha_{sc} = \frac{4}{1 + \left(\frac{r_w}{r_2}\right)^2 + \frac{k_2}{k_1}\left[1 - \left(\frac{r_w}{r_2}\right)^2\right]} \tag{11}$$

where α_{sc} is the convergence factor for a screened well (dimensionless), r_w is the inside radius of the well (L), r_2 is the outside radius of the well (L), k_1 is the hydraulic conductivity (or permeability) of well screen (LT^{-1}), k_2 is the hydraulic conductivity (or permeability) of the formation (LT^{-1}). For fractured media, $r_w = r_2$ so Equation 12 simplifies to $\alpha_{sc} = 2$.

Equation 10 can be evaluated using data from IWPVP testing in porous media, as reported by Osorno *et al.* (2018). If the vertical capture distance is assumed the same in the probe and the formation, $z_{pm} = Y_{probe,}$ (see Figure 2.7) we approximate $Y_c = 2d_w = 2(51\ mm) = 102\ mm$. The probe channel height is $(2b)_{probe} = 4.5\ mm$. This leads to a value of q_{probe}/q_{pm} of 23, which is comparable to the modeled value of 18.6 reported by Osorno *et al.* (2018). The

difference might be attributable to an overestimate of Y_c by the Ogilvy formula due to the presence of the IWPVP in the well, which is not represented in the formula. Experimentally, Osorno *et al.* (2018) determined the ratio q_{probe}/v_{pm}, where v_{pm} is the seepage velocity in the porous medium outside the well. They reported ratios between 6.17 and 8.44, which are within the expected range if porosity of the porous medium is assumed to be between 0.33 and 0.45, i.e., $q_{probe}/v_{pm} = q_{probe}/q_{pm} * n$.

For fractured media, Equation 8 predicts that the calibration slope varies linearly with the fracture aperture, $(2b)_f$. Equation 11 indicates that as long as $k_2 >> k_1$, Y_c is invariant for a particular well. Under this condition, when the aperture is fixed at 500 μm (0.5 mm), and allowing $Y_c = 2d_w$ = 102 mm, the slope is expected to be about 0.4 (= (0.5 mm * 102 mm)/ (4.5 mm * 27 mm)). Experimentally, a calibration series with q_f varying between 700 cm/d and 8,000 cm/d produced a slope of 0.37, which is in good agreement with the predicted slope. The majority of datapoints also fall inside a ± 25% error envelope (Figure 2.8).

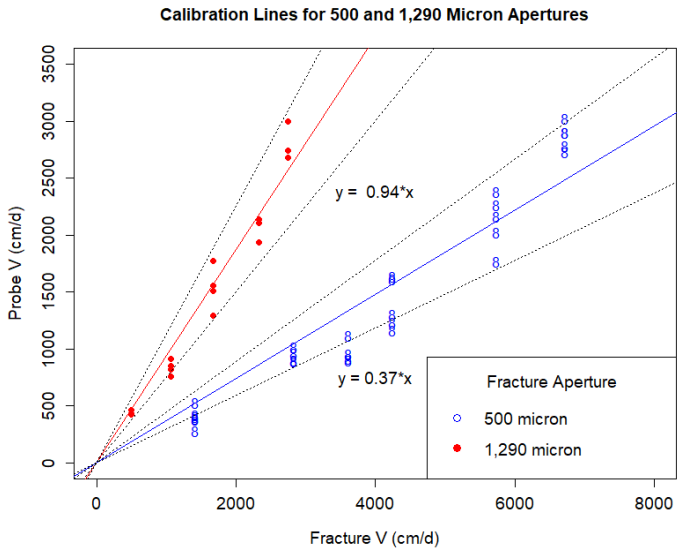

Figure 2.8: The linear relationship between predicated fracture seepage velocity and velocity measured by the probe in a 5 cm diameter well intersecting a 500 µm aperture fracture and 1,290 µm aperture fracture, allowing determination of an experimental calibration factor. Dotted lines indicate ± 25% error of the 0.37 slope and 0.94 slope. R^2 values are 0.97 and 0.99, respectively.

An additional calibration series was undertaken with a fracture aperture of 1290 µm in the FFA. Again, applying Equation 8 the slope of the calibration line was estimated to be 1.1 (= (1.29 mm * 102 mm)/ (4.5 mm * 27 mm)). Experimentally, the slope of the calibration line was found to be 0.94, again in agreement with expectations. Once again, the data points defining the calibration line generally fell within the 25% error envelope (Figure 2.8). The similarity between experimental and estimated calibration factors demonstrates the viability and accuracy of the IWPVP as tool for measuring flow in the laboratory FFA.

2.4.4 – Flow Direction Determination

The IWPVP is, in principle, able to determine flow direction in addition to magnitude. An assessment of the IWPVP flow direction measurements for the fractured media application was made in a series of tests in which q_f was fixed at 4,000 cm/d, the fracture aperture was set to

500 µm, and the IWPVP was systematically rotated by 10˚, establishing a total arc of 90˚. For practical reasons, the absolute direction of flow within the FFA was unchanging. The effect of a changing flow direction was achieved by changing the orientation of the probe inside the FFA. Equation 3 was applied to determine the flow direction angle relative to a predetermined channel on the probe. The test series demonstrated that the probe was generally able to predict flow direction correctly to within about ± 15°, performance is comparable to the ± 15° reported by Osorno *et al.* (2018) for the probe in porous media (Table 1; Figure 2.9). However, it was noted that flow traveling within 10° of a straight path through the probe exhibited a slightly greater uncertainty, estimated to be ± 20°. It is noted that there appears to be a trend in the data that suggests the lower flow angles are overestimated while higher flow angles are underestimated. Further testing would need to be conducted to determine if this is a consistent trend and the potential reasoning behind it.

Table 2: Table of probe orientations relative to flow direction and the calculated flow direction from probe breakthrough curves. Expected flow angle was estimated visually in FFA.

Expected flow angle in degrees	Measured angle in degrees (IWPVP) (± indicate one standard deviation)
0	0 ± 0
10	0 ± 0
20	33 ± 1
30	42 ± 1
40	40 ± 0
50	47 ± 3
60	47 ± 4
70	57 ± 1
80	90 ± 0
90	90 ± 0

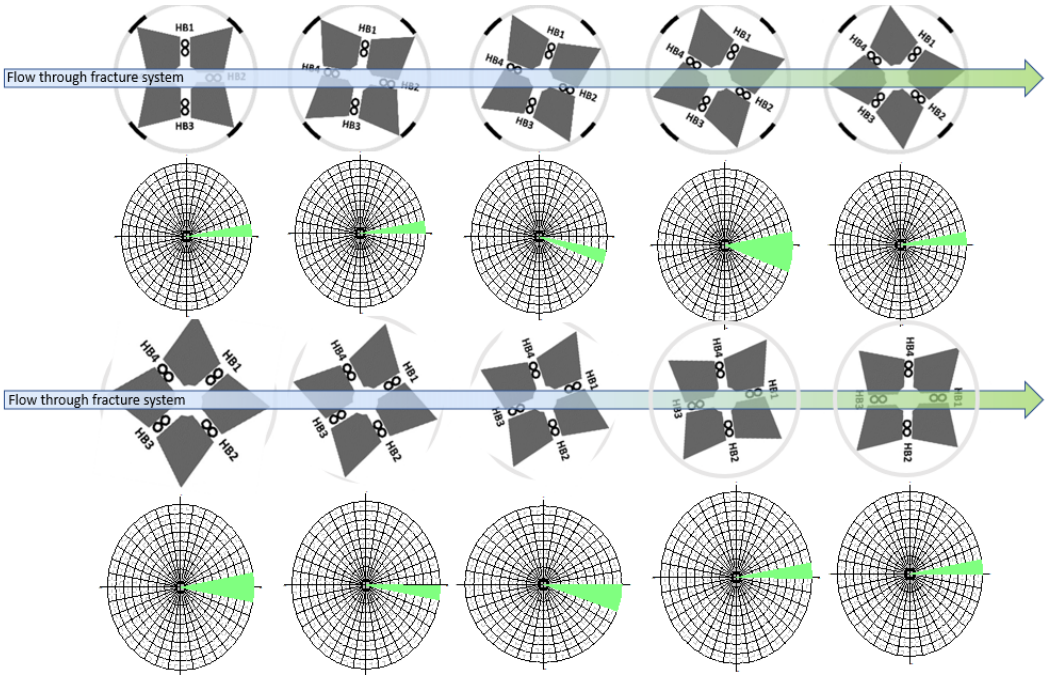

Figure 2.9: Visual representation of probe orientation change and estimated flow direction

2.5 – Conclusions

On the basis of close agreement between calculated and experimental testing results, it is concluded that the FFA established near-ideal conditions representative of a single fracture conducting water flow. Laboratory testing of the IWPVP demonstrated that the best probe performance was achieved when small volumes of tracer were delivered to the center of the probe's mixing chamber. A modified injection system enhanced IWPVP performance for both saline tracers and deionized water.

It is further concluded from this work that the IWPVP performs well for the quantification of horizontal water flux through single fractures. The flux measured within the probe responds linearly to flow in surrounding fractures up to about q_f = 80 m/d. Moreover, under idealized conditions, the probe is capable of quantifying flow directions within about ± 20°. This level of confidence in flow directions may not be achievable in all field settings, but

assuming good hydraulic connections between the fractures and the borehole (containing the probe), flow directions should be distinguishable at least between quadrants, as indicated by tracer transport out of probe (i.e, ± 45°). Note that these measurements are highly localized, so even with this degree of uncertainty on the flow direction, the data may be quite useful, especially when combined with other localized measurements in order to gain an understanding of larger scale trends.

It is also concluded that if the capture width of a borehole, intersecting a fracture, can be estimated reasonably, and if it may be considered invariant, or minimally variable over a testing period, then the IWPVP response will vary linearly with the fracture aperture. Conversely, if fracture apertures are known from other, independent, sources (e.g. hydraulic tests or borehole logs), then a measured flux in the probe can be used to estimate water flux in an intersecting fracture.

In addition, this work demonstrates the viability of the IWPVP as a tool for characterizing fractured media. The passive nature of the measurements, low cost of assembly and deployment, and speed of testing are important advantages offered by this tool. Future work will involve field deployment of the tool at a fractured rock site and investigation into methods to estimate calibration factors in a field setting, as well as further work to understand the lower end of the calibration lines at slower flow rates.

2.6 – References

Alexander, M., Berg, S.J., Illman, W.A., 2011. Field Study of Hydrogeologic Characterization Methods in a Heterogeneous Aquifer. Ground Water 49, 365–382. https://doi.org/10.1111/j.1745-6584.2010.00729.x

Annable, M.D., Hatfield, K., Cho, J., Klammler, H., Parker, B.L., Cherry, J.A., Rao, P.S.C., 2005. Field-scale evaluation of the passive flux meter for simultaneous measurement of

groundwater and contaminant fluxes. Environ. Sci. Technol. 39, 7194–7201. https://doi.org/10.1021/es050074g

Berkowitz, B., 2002. Characterizing flow and transport in fractured geological media : A review. Adv. Water Resour. 25, 861–884. https://doi.org/https://doi.org/10.1016/S0309-1708(02)00042-8

Bianchi, M., Zheng, C., Tick, G.R., Gorelick, S.M., 2011. Investigation of small-scale preferential flow with a forced-gradient tracer test. Ground Water 49, 503–514. https://doi.org/10.1111/j.1745-6584.2010.00746.x

Butler, J.J., Dietrich, P., Wittig, V., Christy, T., 2007. Characterizing hydraulic conductivity with the direct-push permeameter. Ground Water 45, 409–419. https://doi.org/10.1111/j.1745-6584.2007.00300.x

Cacas, M.C., Ledoux, E., de Marsily, G., Tillie, B., Barbreau, A., Durand, E., Feuga, B., Peaudecerf, P., 1990. Modeling fracture flow with a stochastic discrete fracture network: calibration and validation: 1. The flow model. Water Resour. Res. 26, 479–489. https://doi.org/10.1029/WR026i003p00479

Cherry, J.A., Parker, B.L., Keller, C., 2007. A new depth-discrete multilevel monitoring approach for fractured rock. Gr. Water Monit. Remediat. 27, 57–70. https://doi.org/10.1111/j.1745-6592.2007.00137.x

Devlin, J.F., McElwee, C.D., 2007. Effects of measurement error on horizontal hydraulic gradient estimates. Ground Water 45, 62–73. https://doi.org/10.1111/j.1745-6584.2006.00249.x

Devlin, J.F., Tsoflias, G., McGlashan, M., Schillig, P., 2009. An inexpensive multilevel array of sensors for direct ground water velocity measurement. Gr. Water Monit. Remediat. 29, 73–77. https://doi.org/10.1111/j.1745-6592.2009.01233.x

Feenstra, S., Cherry, J.A., Sudicky, E.A., Haq, Z., 1984. Matrix Diffusion Effects on Contaminant Migration from an Injection Well in Fractured Sandstone. Ground Water 22, 307–316. https://doi.org/10.1111/j.1745-6584.1984.tb01403.x

Gernand, J.D., Heidtman, J.P., 1997. Detailed Pumping Test to Characterize a Fractured Bedrock Aquifer. Ground Water 35, 632–637. https://doi.org/10.1111/j.1745-6584.1997.tb00128.x

Halevy, E., Moser, H., Zellhofer, O., Zuber, A. 1967. Borehole Dilution Techniques: A Critical Review. In: Isotopes in Hydrology, IAEA, Vienna, Austria, p 531-564.

Hatfield, K., Annable, M., Cho, J., Rao, P.S.C., Klammler, H., 2004. A direct passive method for measuring water and contaminant fluxes in porous media. J. Contam. Hydrol. 75, 155–181. https://doi.org/10.1016/j.jconhyd.2004.06.005

Heyer, B., Osorno, T.C., Carrera, Mok, C.M. B., Devlin, J.F. 2019. Application of the In-Well Point Velocity Probe (IWPVP) in Fractured Media. Annual GSA meeting, Phoenix, Arizona, September 22-25.

ITRC, 2010. Use and Measurement of Mass Flux and Mass Discharge. ITRC Technol. Overv. MASSFLUX-1, 1–154.

Johnson, C.R., Greenkorn, J.A., and Woods, E.G. 1966. Pulse testing, a new method for describing reservoir flow properties between wells, J. Pet. Technol., 18, 1599-1604.

Klammler, H., Hatfield, K., Newman, M.A., Cho, J., Annable, M.D., Parker, B.L., Cherry, J.A., Perminova, I., 2016. A new device for characterizing fracture networks and measuring groundwater and contaminant fluxes in fractured rock aquifers. Water Resour. Res. 52, 5400–5420. https://doi.org/10.1002/2015WR018389

Landstrom, O., Klockars, C., Persson, O., Andersson, K., Torstenfelt, B., Allard, B., Tullborg, E., Larsson, S., 1983. Migration Experiments in Studsvik. KBS Nucl. Fuel Saf. Proj., Stock. Tech. Rep.

Maldaner, C.H., Munn, J.D., Coleman, T.I., Molson, J.W., Parker, B.L., 2019. Groundwater Flow Quantification in Fractured Rock Boreholes Using Active Distributed Temperature Sensing Under Natural Gradient Conditions. Water Resour. Res. 55, 3285–3306. https://doi.org/10.1029/2018WR024319

Novakowski, K.S., 1989. A composite analytical model for analysis of pumping tests affected by well bore storage and finite thickness skin. Water Resour. Res. 25, 1937–1946. https://doi.org/10.1029/WR025i009p01937

Novakowski, K.S., 1990. ANALYSIS OF AQUIFER TESTS CONDUCTED IN FRACTURED ROCK: A REVIEW OF THE PHYSICAL BACKGROUND AND THE DESIGN OF A COMPUTER PROGRAM FOR GENERATING TYPE CURVES. Groundwater 28, 99–107. https://doi.org/10.1111/j.1745-6584.1990.tb02233.x

Novakowski, K., Bickerton, G., Lapcevic, P., Voralek, J., Ross, N., 2006. Measurements of groundwater velocity in discrete rock fractures. J. Contam. Hydrol. 82, 44–60. https://doi.org/10.1016/j.jconhyd.2005.09.001

Novakowski, K.S., Evans, G. V., Lever, D.A., Raven, K.G., 1985. A Field Example of Measuring Hydrodynamic Dispersion in a Single Fracture. Water Resour. Res. 21, 1165–1174. https://doi.org/10.1029/WR021i008p01165

Ogilvi, N.A. 1958. Elektroliceskij metod opredelenija skorostej filtracii. Bjull. O. N. T. I . no.4, Gosgeoltehizdat.

Osorno, T.C., Devlin, J.F., Firdous, R., 2018. An In-Well Point Velocity Probe for the rapid determination of groundwater velocity at the centimeter-scale. J. Hydrol. 557, 539–546. https://doi.org/10.1016/j.jhydrol.2017.12.033

Osorno, T.C., Devlin, J.F., Cormican, A., Heyer, B., Jones, M. 2020. Progress Update Report on IWPVP and PVP Data Analysis for Neodesha, KS, November 2019. Addendum to the Biosparge Pilot Test and Amendment Injection Workplan submitted by Sovereign Consulting Inc. to the Kansas Department of Health and Environment, May, 11 pp.

Parker, B.L., Cherry, J.A., Chapman, S.W., 2012. Discrete Fracture Network Approach for Studying Contamination in Fractured Rock. AQUA mundi 101–116. https://doi.org/10.4409/Am-052-12-0046

Post, V.E.A., von Asmuth, J.R., 2013. Review: Hydraulic head measurements—new technologies, classic pitfalls. Hydrogeol. J. 21, 737–750. https://doi.org/10.1007/s10040-013-0969-0

Ricciardi, K.L., Pinder, G.F., Karatzas, G.P., 2009. Efficient Groundwater Remediation System Designs with Flow and Concentration Constraints Subject to Uncertainty. J. Water Resour. Plan. Manag. 135, 128–137. https://doi.org/10.1061/(asce)0733-9496(2009)135:2(128)

Schillig, P.C., 2012. VelProbePE: An automated spreadsheet program for interpreting point velocity probe breakthrough curves. Comput. Geosci. 39, 161–170. https://doi.org/10.1016/j.cageo.2011.06.007

Schillig, P.C. & Devlin, J.F., 2018. VELPROBE 3.1 BETA-d, www.people.ku.edu/~jfdevlin/software.html, accessed Sept. 15, 2020.

Schillig, P.C., Devlin, J.F., Rudolph, D., 2016. Upscaling Point Velocity Measurements to Characterize a Glacial Outwash Aquifer. Groundwater 54, 394–405. https://doi.org/10.1111/gwat.12357

Shapiro, A.M., 2002. Cautions and Suggestions for Geochemical Sampling in Fractured Rock. Groundw. Monit. Remediat. 22, 151–164. https://doi.org/10.1111/j.1745-6592.2002.tb00764.x

Sterling, S.N., Parker, B.L., Cherry, J.A., Williams, J.H., Lane, J.W., Haeni, F.P., 2005. Vertical cross contamination of trichloroethylene in a borehole in fractured sandstone. Ground Water 43, 557–573. https://doi.org/10.1111/j.1745-6584.2005.0087.x

Sudicky, E.A., 1986. A natural gradient experiment on solute transport in a sand aquifer: Spatial variability of hydraulic conductivity and its role in the dispersion process. Water Resour. Res. 22, 2069–2082. https://doi.org/10.1029/WR022i013p02069

Tester, J.W., Bivins, R.L., Potter, R.M., 1982. Interwell Tracer Analyses of a Hydraulically Fractured Granitic Geothermal Reservoir. Soc. Pet. Eng. J. 22, 537–554. https://doi.org/10.2118/8270-PA

Tsoflias, G.P., Van Gestel, J.P., Stoffa, P.L., Blankenship, D.D., Sen, M., 2004. Vertical fracture detection by exploiting the polarization properties of ground-penetrating radar signals. Geophysics 69, 803–810. https://doi.org/10.1190/1.1759466

Wilson, J.T., Mandell, W.A., Paillet, F.L., Bayless, E.R., Hanson, R.T., Kearl, P.M., Kerfoot, W.B., Newhouse, M.W., Pedler, W.H., 2001. An evaluation of borehole flowmeters used to measure horizontal ground-water flow in limestones of Indiana, Kentucky, and Tennessee, 1999. https://doi.org/https://doi.org/10.3133/wri014139

Zimmerman, R.W., Bodvarsson, G.S., 1996. Hydraulic conductivity of rock fractures. Transp. Porous Media 23, 1–30. https://doi.org/10.1007/BF00145263

3.0 – Water Flux Depth Profiling in Fractured Rock with an In-Well Point Velocity Probe (IWPVP)

3.1 – Abstract

Flow in a fractured rock aquifer beneath the Edwards Air Force Base, California, was characterized by depth profiling two wells with In-Well Point Velocity Probes (IWPVPs). The probes, which were originally designed for use in porous media wells, were modified for use in fractured rock wells and to meet the challenges of up to 38 m sampling depths, high background salinity of the water, and the diameters and construction of the wells. The In-Well Point Velocity Probe measures groundwater fluxes inside the probe, and these are converted to fluxes in the aquifer through calibration curves. At this site, the internal fluxes were measured over the range of 300 – 5,300 cm/d and determined flow directions generally consistent with the expected regional flow direction. However, the flow altered most notably following a rain event (up to 180° change in direction). The IWPVP was able to identify highly transmissive zones in the fractured rock, which were independently confirmed by passive flux meters, oxidation-reduction sensors, and transmissivities determined during a FLUTe liner deployment. With additional information on fracture apertures in select locations from an acoustic televiewer, the measured internal fluxes were used to estimate water fluxes in the fractures with values ranging between 370 cm/d – 2,239 cm/d.

3.2 – Introduction

Conventionally, flow in fractured rock is characterized by performing hydraulic tests to permit the estimation of empirical, effective aquifer parameters, including fracture hydraulic conductivity (K_f), porosity (n_f), hydraulic gradient, and fracture aperture ($2b$). These values are used in a form of Darcy's Law, derived from the Cubic Law, to relate flow rates to hydraulic gradients in the fractures. However, unless the fracture density is sufficient to satisfy an

equivalent porous medium assumption (van der Kamp, 1992; Ghasemizadeh *et al.*, 2015), Darcy calculations based on hydraulic head measurements from wells can result in misleading predictions of groundwater velocity – due both to the discrete nature of the fractures and the inherent limitations of the Darcy approach (Alexander *et al.*, 2007; Butler *et al.*, 2007; Devlin & McElwee, 2007; Ricciardi *et al.*, 2009; Post & von Asmuth, 2013). In addition, hydraulic testing commonly involves pumping or pressurization of some portion of a borehole that can dilate or otherwise alter fractures, biasing the estimates of K_f, n_f, and $2b$ (Novakowski *et al.*, 1985; Parker *et al.*, 2012). Also, these tests may be unreliable when performed in open boreholes where flow across depths occurs – i.e. between fractures not normally connected hydraulically – which does not represent ambient flow conditions. This can lead to underestimated solute spreading predictions (Berkowitz, 2002). The interpretation of hydraulic tests in fractured rock therefore requires a high level of specialized training.

The need for simple, effective, and reliable tools to analyze flow in fractured media is driving the development of new technologies with the various aims of identifying fracture occurrences in boreholes and measuring flow rates within them, without reference to the empirical parameters needed for Darcy's Law calculations. Examples of such technologies include the fractured rock passive flux meter (FRPFM), which adapts the passive flux meter (PFM, Hatfield *et al.*, 2004) to fractured rock settings (Klammler *et al.*, 2016), and flexible impervious liners (FLUTe™, http://www.flute.com), which have been adapted to measure transmissivity as a function of depth during installation (Keller *et al.*, 2014). The FLUTe liner has the added benefit of sealing the borehole in which it is deployed, preventing cross-depth flow. FLUTe liners have also been used to support depth-specific temperature measurements from which zones of active groundwater flow can be identified (Shapiro, 2002; Novakowski *et*

al., 2006; Cherry *et al*., 2007; Pehme *et al.*, 2010). A comprehensive approach for fractured rock characterization, the Discrete Fracture Network (DFN) approach, has been developed to guide decision making for the selection of hydraulic and borehole methods to apply in fractured media investigations (Parker *et al.*, 2012).

A more recent technology that shows promise for use in characterizing fracture flow is the In-Well Point Velocity Probe (IWPVP). This instrument has been shown to provide useful horizontal flow directions and magnitudes from porous media wells both in the laboratory (Osorno *et al*., 2018) and the field (Osorno *et al*., 2020). Briefly, the IWPVP consists of a cylindrical probe through which two perpendicular, intersecting channels run. Water is captured by funnel-shaped inlets at the outside ends of the up-stream channels and directed through the middle of the probe to the downstream ends of the channels. Tracer is introduced at the intersection of the channels (the mixing chamber) and is carried through the channels and over wire pairs that monitor changes in electrical resistance in response to the tracer movement (Figure 3.1). The resulting signals can then be interpreted to provide information on both flow magnitude and direction. The IWPVP's channels are about 3 cm in height, making the probe small enough to measure flow in single fractures in rock (or other media), or closely spaced fracture sets.

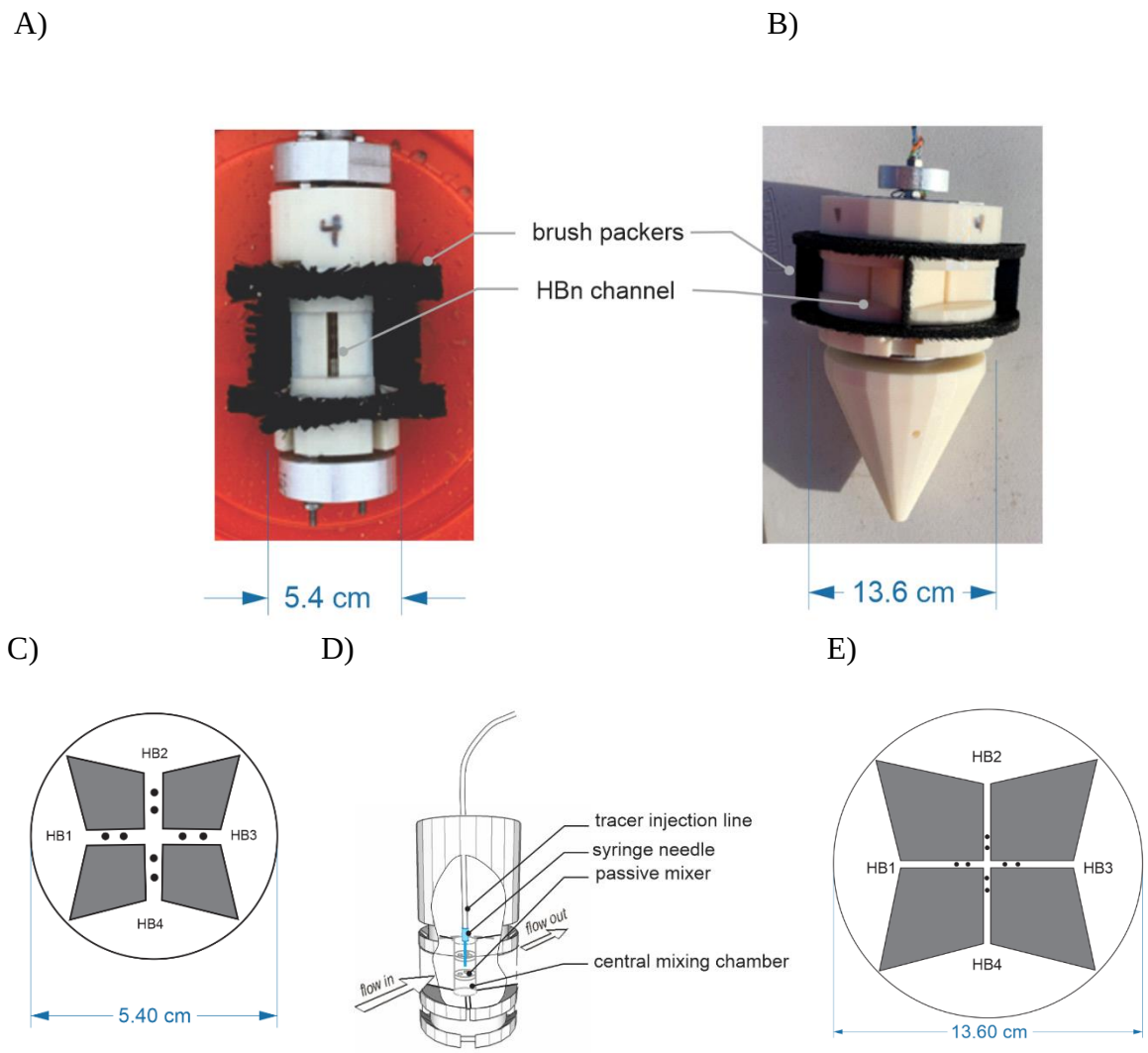

Figure 3.1: IWPVPs used in the current study. A) the unit used in the 5.4 cm diameter borehole. B) the unit used in the 13.6 cm diameter borehole. The pointed tip was added to aid the probe descend past a joint in the telescoping borehole (larger diameter in the upper 9 m). C) plan view section showing positions of detector wires in the 5.4 cm diameter probe. D) cut-away view of IWPVP showing position of needle for tracer delivery in the center of the mixing chamber. E) plan view section showing positions of detector wires in the 13.6 cm diameter probe.

To test the hypothesis that IWPVPs were suitable for use in fractured media, laboratory testing was undertaken (Heyer *et al.*, in review). A fracture flow apparatus (FFA) was constructed to mimic a single, horizontal fracture. The FFA was equipped with a mock well allowing deployment of an IWPVP across the simulated fracture. By varying flow rates through the FFA and comparing known water fluxes in the fracture (q_f) to fluxes measured inside the

probe (q_p), calibration factors could be determined ($\alpha_c = q_f / q_p$). These factors depended on the effective aperture of the fracture. Also, the laboratory work demonstrated that the IWPVP could detect flow direction within about ± 15°. These encouraging findings led to further testing of the probe in field fractured rock wells. The purpose of this work is to evaluate the IWPVP performance in fractured rock boreholes for its ability to identify the locations of fractures intersecting the borehole and provide estimates of the associated water fluxes and directions of flow.

3.3 – Field Site

The work was conducted at the Edwards Air Force Base in California (Figure 3.2). Groundwater flow in bedrock fractures was measured in two boreholes (IW-01 and IBH-1) over the depth range 17 m to 38 m below ground surface (bgs). The boreholes, which were previously installed by GSI Environmental Inc. (hereafter referred to as GSI) for use in a tracer test, were completed as part of a plume management plan for the site. The groundwater at the site is known to contain chlorinated ethenes associated with aircraft maintenance and repair. The plume extends south and eastward (~150° clockwise from N), consistent with general expectations, based on the regional flow, documented by Dutcher *et al.* (1963) (Figure 3.2). The first borehole (IW-01) was drilled with 7.6 cm (3-inch) diameter PVC screen installed to a depth of about 43 m below ground surface. The second borehole (IBH-1) was drilled and cased with a diameter of 22.9 cm (9 inches) to a depth of 9 m, where the borehole was telescoped down to about 15.8 cm (6.25 inches) diameter and completed to a depth of about 43 m without casing.

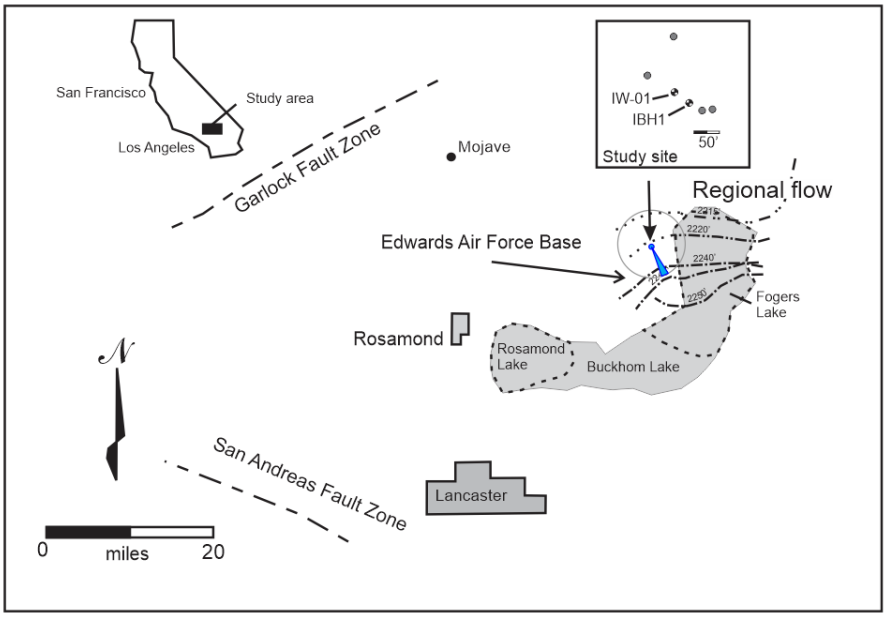

Figure 3.2: Location and regional hydrogeology of the study area. Regional flow in the vicinity of the study site is south-southeast (blue vector; approximately 150° clockwise from north) according to Dutcher et al. (1963)

The bedrock at the site is classified as the basement complex by Dutcher *et al.* (1963) and consists of deeply weathered granites that can be locally unconsolidated. Wells in this formation yield only small quantities of water. GSI described the rock as granitic to dioritic with a strong phaneritic texture and mineralogy consisting of quartz, feldspar, hornblende, and muscovite/biotite.

3.4 – Methods

3.4.1 – GSI Instrumentation of the Site

Prior to the deployment of the IWPVPs, GSI used a variety of tools in IW-01, IBH-1, and neighboring wells. They installed a FLUTe liner in IBH-1 and profiled the transmissivity of the formation as a function of depth. Depth profiles for fracture identification were also obtained from oxidation-reduction potential (ORP) sensors suspended in IW-01. In addition, a string of

passive flux meters (PFM) was suspended in IW-01 for a period of about three weeks to obtain time-averaged, depth-specific estimates of groundwater flux.

3.4.2 – IWPVP Instrumentation

The IWPVP fieldwork was carried out early in 2019. The IWPVPs were sized according to the wells in which they were deployed. They were fabricated with a U-Print 3D printer and acrylonitrile butadiene styrene (ABS) plastic (Figure 3.1). The interior dimensions of the tracer detection systems were common to both designs, i.e., detector wire pairs were positioned at the same distances from the probe center in each case, and the detector channels were of identical widths (See HBn channels in Figure 3.1 A,B). This design has previously been demonstrated to detect flow internally within the probe with a flux of at least 100 cm/d. Lower flows could not be produced in the lab tests to define lower detection limit. However, the channel lengths, funnel sizes, and overall diameters of the probe bodies were customized to fit the boreholes with a small amount of annular space that was filled with brush packers. The brush packers did not create perfect seals, but they did create relatively low permeability barriers that separated the probe funnels from one another and contributed to some isolation of the probe vertically within the borehole. The permeability contrast between the brushes and the open channels in the probe promoted flow through the probe, rather than around it, during a test. A notable limitation of the brush-seal design is that vertical flow in a borehole is not entirely prevented, potentially producing responses in the probe that interfere with responses due to purely horizontal flow. In some applications, most notably those where vertical flow rates in the boreholes are very high, the IWPVP may require inflatable packers to fully isolate a test zone and properly quantify horizontal flow. For the purposes of this project, the brush-seals appeared to perform satisfactorily and facilitated probe placement and re-positioning in test boreholes and to evaluate their performance in a field setting (Figure 3.1 A,B). The brushes were cut to a length of 1.9 cm,

which was of sufficient length to provide the flexibility needed for positioning of the IWPVP in the borehole, without risk of inadvertently lodging and trapping the instrument downhole.

The probes were lowered into place on 0.95 cm diameter stainless steel rods joined with stainless steel screw-connectors. The plastic probe bodies were sandwiched between two disc-shaped steel brackets on the top and bottom of the probe bodies and held in place with extension screws (running through the probe bodies). The brackets provided the strength required to maintain probe integrity during the probe positioning maneuvers over the 38 m descent into, and recovery from, the borehole.

To ensure that the probes remained centered and fully vertical in the wells during deployment and measurements, centralizers, consisting of three ~1 m long 3.175 mm diameter spring steel wire, were fashioned to spring outward and contact the test borehole walls, mounted on the central rod to which the probe was also attached (Figure 3.3).

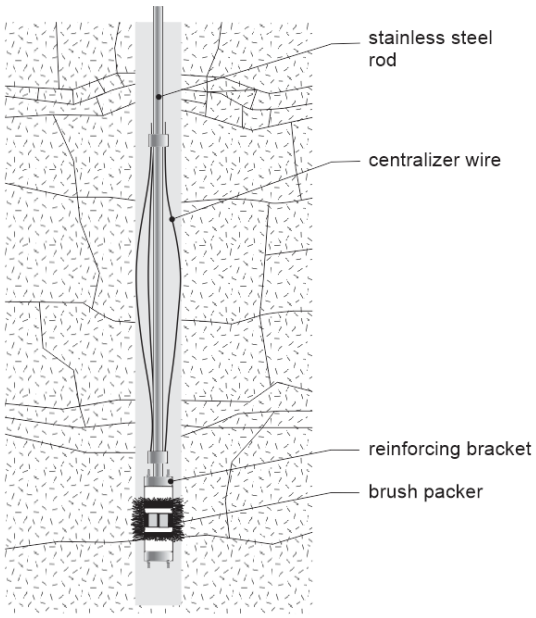

Figure 3.3: Schematic view of an IWPVP in a borehole showing the brush packers, reinforcing brackets, and spring-loaded centralizer wires.

3.4.3 – Procedures

Upon arriving on-site at Edwards AFB, the probes (with their respective reinforcing brackets, central rods, and centralizer wires) were fully assembled on the surface and the detector wiring and tracer lines were fed through the steel rods. Each rod was marked so the compass orientation of the probe was always known at the ground surface as the probe was moved down the borehole. A marking was also applied to top of the well casing to help ensure the probe maintained the same orientation for all measurements. No rotational torque was applied to the assembly during emplacement. Tests were conducted sequentially, progressing from the bottoms of the wells upward at predetermined intervals selected on the basis of expected zones of water flow.

Deionized water (DI) was selected as the IWPVP tracer because it exhibited a measurable conductivity contrast with the background groundwater, which had an electrical conductance on the order of 200 $\mu S\ cm^{-1}$ and with the added advantage of posing no regulatory concern. Each time the probe was repositioned in the borehole, a tracer volume of about 5 to 7 mL was injected downhole to ensure the tracer solution was continuous throughout the injection line from the surface to the central mixing chamber in the probe (Figure 3.1D). This volume of DI generally produced signals from all four channels in the probe, confirming proper operation of the electronics and injection line. At this site, the probe cleared of excess tracer rapidly (< 10 minutes) and testing could begin. The actual testing was conducted with injections of between 0.2 mL to 2 mL, which resulted in dominant signals appearing in only one or two channels of the probe, as expected. All tests were repeated at least twice, and in several locations, additional tracer injections were performed with various volumes to confirm that the signals were correctly

identified. Following testing at a particular depth, the probe was repositioned at the next desired sampling depth and the procedure was repeated.

The 7.62 cm screened well (IW-01) was characterized in a single day, from depths of 38 m to 25 m, at intervals of about 1.5 m and from 25 m to 18 m in 0.6 m intervals, reflecting the anticipated zones of highest fracture density suggested by prior work, including the FLUTe liner installation. After decontamination of the rods and lines, the larger probe was attached to the lead rod, and the 15.9 cm uncased well (IBH-1) was profiled over the course of the next three days. The longer execution time was due to in part to time spent decontaminating the equipment and in part to a rain delay midway through the procedure (1.88 cm of precipitation). In addition, the larger well was subjected to an increased number of tests. The 18 m to 25 m depths were characterized at 0.6 m intervals on day 1. On day 2, after the rain event, 2 locations of interest (18.9 m and 16.5 m), identified during FLUTe deployment, were tested. The depth interval 38 m to 21 m was profiled at 1.5 m intervals on day 3.

3.4.4 – Data Analysis

IWPVP data, in the form of tracer breakthrough curves, were analyzed using VelprobePE 3.1 beta d (Schillig, 2012; Schillig and Devlin, 2018), which estimates flux on the basis of either curve fitting or method of moments calculations. In some tests, the signals manifested as two closely spaced peaks. Laboratory work indicated that in such cases the first peaks were more reliably a linear function of flux (Heyer *et al.*, in review). As discussed in Heyer *et al.*, the ratio of flux in a fracture to that in the probe is given by

$$\frac{q_1}{q_2} = \frac{B_2 2b_2}{B_1 2b_1} \qquad (1)$$

where, q_2 is the water flux in the probe (LT^{-1}), q_1 is the water flux in the fracture (LT^{-1}), B_1 is the capture width the probe exerts in the fracture (L), B_2 is the height of the channels in the probe

(2.7 cm), $2b_1$ is the aperture of the fracture (L) and $2b_2$ is the width of a channels in the probe (0.45 cm). Because information on the fracture apertures was not known *a priori*, the measured fluxes could not immediately be converted to fluxes in the fracture rock aquifer (Equation 1). However, relative depth-specific apparent fluxes were readily discernible. In cases where signals were observed in two probe channels, the horizontal flow direction in the aquifer, referenced to a pre-selected channel in the probe (corresponding to marks on the rods running to the surface), was interpreted as described by Osorno (2018) and subsequently related to magnetic north using the directional marks on the well casing and a compass (Equation 2). The magnetic declination of the area, 12°, was then taken into account to convert the direction relative to geographic north. Determining the apparent angle of flow relative to the dominant flow channel (θ_{app}) involves both the estimated velocities through two channels ($v_{1,2}$) and the mass fraction weights of the tracer/area under the BTCs ($W_{1,2}$).

$$\theta_{app} = tan^{-1}\frac{(v_1)W_1}{(v_2)W_2} \quad (2)$$

3.4.5 Estimation of Water Flux in the Fractures

Several months after the field campaign, acoustic borehole televiewer (ATV) data were acquired from IBH-1 by GSI. With this dataset it was possible to visually identify some fractures that intersected the borehole and measure their aperture sizes at the borehole walls. Note that these visible apertures are not necessarily representative of apertures in the aquifer removed from the borehole. In many cases they might be enlarged due to pressure relief or chipping of the borehole wall during drilling. So, uncertainty exists in any interpretations using these observations. Nevertheless, the apertures determined with the ATV provide a starting point for any assessment that can be refined with subsequent data from hydraulic or other forms of testing.

The ATV was reported to have a fracture aperture detection limit of about 2,500 μm (Pacific Surveys, www.pacificsurveys.com). With this in mind, fracture apertures documented in IBH-1 with the ATV ranged from 2,500 μm to 14,000 μm in size; smaller aperture fractures that may have been present and hydraulically active were not observable. Following the approach of Heyer *et al.* (in review), a single fracture parallel plate model was used to relate capture zone width to fracture aperture. With this information applied to the uncased well IBH-1, along with field flux measurements, the effective water fluxes in the fractures were estimated.

3.5 – Results

3.5.1 – IWPVP Depth Profiles of Flux

To assess the trends in relative horizontal flux as a function of depth, all IWPVP test results were initially examined as apparent fluxes, i.e., those measured in the probe without conversion to in-fracture fluxes. In borehole IW-01, flow was detected at every depth tested shallower than 36.5 m bgs (Figure 3.4A). Point-specific apparent fluxes between about 300 cm/d and 1,250 cm/d were observed from depths of 18 m to 29 m. At depths greater than 30 m, flow rates observed were generally greater, with the highest flux (2,467 cm/d) measured at 31 m bgs. However, no detectable flow was observed at 36.5 m.

In uncased borehole IBH-1, water flow was detected at all sampled depths except 19.8 m and 22 m bgs (Figure 3.4B). In general, the apparent flux was slightly more variable with depth than had been observed at IW-01, with a range of about 400 cm/d to 5,300 cm/d.

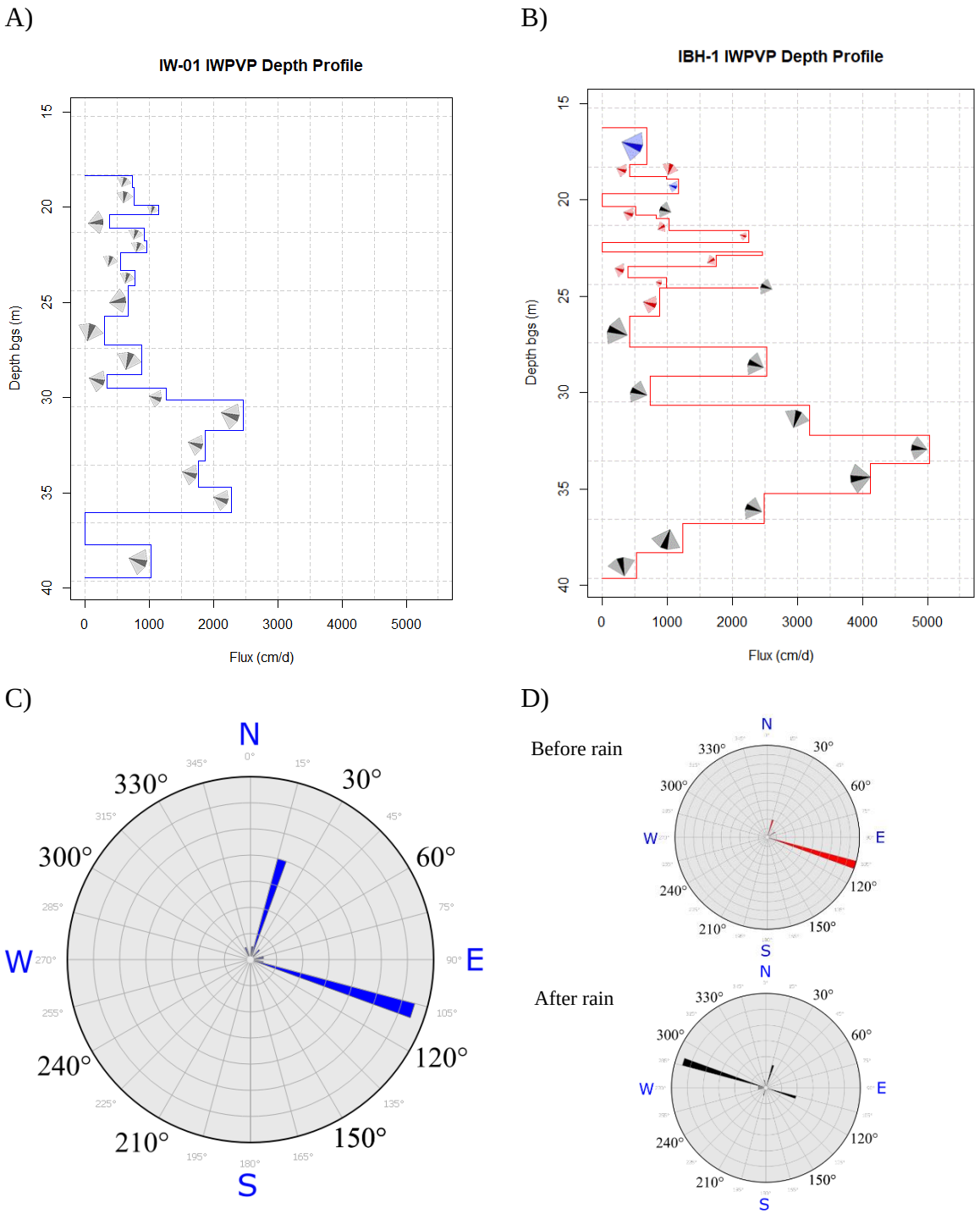

Figure 3.4: Depth profiles of flux measurements (averaged values from two to four tests) and flow direction estimations made inside the IWPVP for A) cased well; IW-01 B) uncased well; IBH-1. Darker shaded areas of direction indicators represent the +/- 15° uncertainty determined from laboratory testing and light shaded areas represent the 90° quadrant associated with the channel in which tracer is exiting. C) Rose diagrams of flow directions derived from injections at various depths through IW-01 D) Rose diagrams of flow directions derived from injections at various depths through IBH-1 before the rain event (red) and after the rain event (black)

3.5.2 – IWPVP-Derived Flow Directions

Each flux measurement had a corresponding apparent flow direction (Figure 3.4 A,B). The majority of injections in IW-01 indicated a flow angle between 15° and 110° clockwise from north with the higher angle dominating (Figure 3.4C). This compares favorably to the SSE direction (~150°) generally expected for the region, as reported by Dutcher *et al.* (1963). In the case of borehole IBH-1, flow directions were divided into those that were measured before and those measured after a significant rain event (Figure 3.4D). Because all other variables appeared to remain constant, the precipitation is the apparent cause of a change in flow direction of about 180°.

3.5.3 – Comparisons with Other Methods

A few months prior to the IWPVP work, FLUTe liners were deployed in IBH-1 from which depth-specific transmissivities were determined (Figure 3.5). The FLUTe method identified zones of relatively high transmissivity at 22 m, 28 m, and 38m bgs and zones of very low transmissivity at 21 m bgs and 24 m bgs. Oxidation-reduction potentials (ORP) were profiled in IW-01. ORP is sensitive to flow distribution when redox-sensitive substances, such as dissolved oxygen, are carried at different concentrations by the groundwater in zones of differing velocity. Under such conditions, variations in ORP with depth signify zones of differing flow rates (Figure 3.5). In this case, zones in a state of relative high oxidation were interpreted as zones of high velocity, where dissolved oxygen could penetrate farther before being reduced biologically or by reactions with chemically reduced mineral phases in the rock. The highest flow rates appeared to be at depths of about 22 m, 28 m, and 34 – 37 m bgs, while the lowest apparent flow rates were identified at 27 m and 37 m bgs, in general agreement with the IWPVP profiles. Additionally, a string of passive flux meters was deployed in IW-01 and left in place for about three weeks beginning immediately after the IWPVP instrumentation was removed from

the borehole. The PFM provided time-averaged depth-specific Darcy fluxes (Figure 3.5). In this case, relatively high rates of flow were identified at depths of about 24 m, 32 – 35 m, and 39 m bgs and relatively low rates at 26 – 29 m, and 35 – 38 m bgs. Once again, the identified depths of high and low flow rates determined by the various methods compare favorably. The time-averaged nature of the PFM data, and the somewhat larger sampling interval led to less pronounced contrasts between the fluxes at various depths. Nevertheless, even in this case, the general trends in flow rate with depth were similar to those identified by other methods.

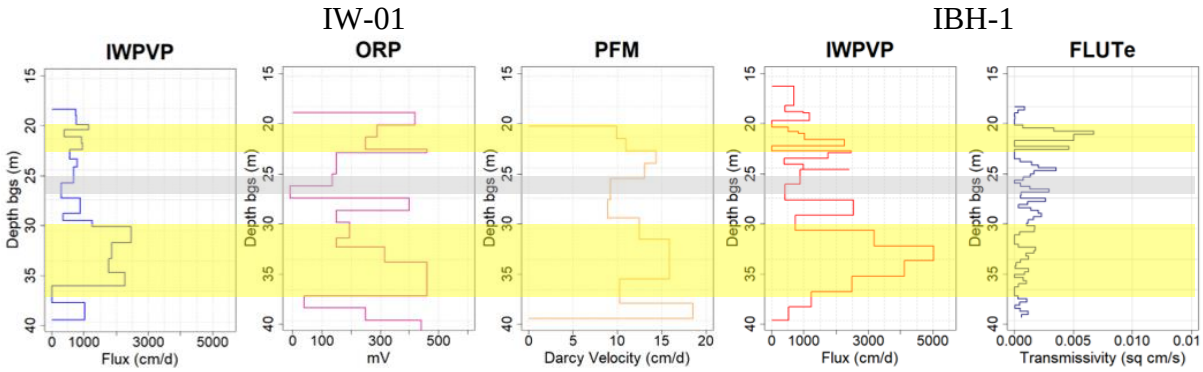

Figure 3.5: Comparison of depth profiles for each tool used on site in both IW-01 and IBH-1. Highlighted areas indicate similar trends in rate of flow between profiles (yellow indicates high flux zones, grey indicates lower flux zones)

3.5.4 – Preliminary Estimation of Flow in the Aquifer

Equation 1 can be used to estimate water fluxes in an aquifer from in probe fluxes if the capture zone size of the well is known (Figure 3.6). This condition was met at five locations where both IWPVP tests and acoustic borehole televiewer logs identified open fractures with measurable apertures. The physical apertures of these fractures ranged from about 7,500 to 12,000 µm. Using apertures ranging from the detection limit of the televiewer (~2,500 µm) to the greatest size recorded in IBH-1 (12,000 µm), the capture zone widths of the well containing the probe could be modeled following the method described by Heyer *et al.* (in review) (Figure 3.6 A-E). A relationship between aperture size and capture zone width was determined and could be

utilized in Equation 1 to understand the relationship between aperture size and calibration factor (Figure 3.6 E,F). The resulting calibration factors for the relevant range of apertures ranged between 0.783 and 0.991. Application of these factors yielded fluxes in the fractures that were slightly less than those measured inside the probe (Figure 3.7). Fluxes of 392 cm/d – 2,397 cm/d inside the probe correspond to 370 cm/d – 2,239 cm/d in the fractures.

A) 2b = 2,250 µm; B = 13.2 cm

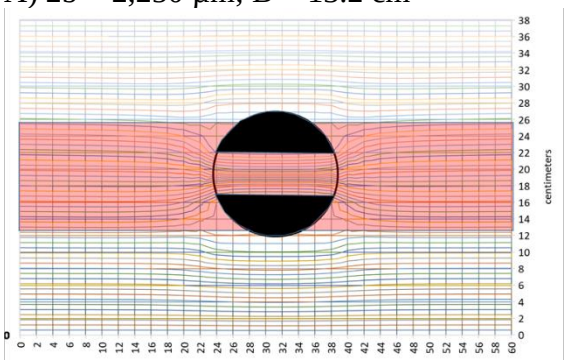

B) 2b = 4,000 µm; B = 7.40 cm

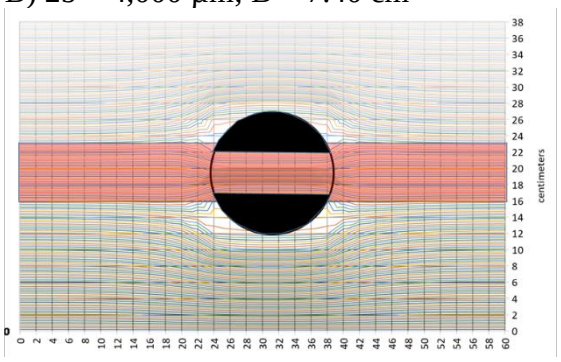

C) 2b = 7,000 µm; B = 3.84 cm

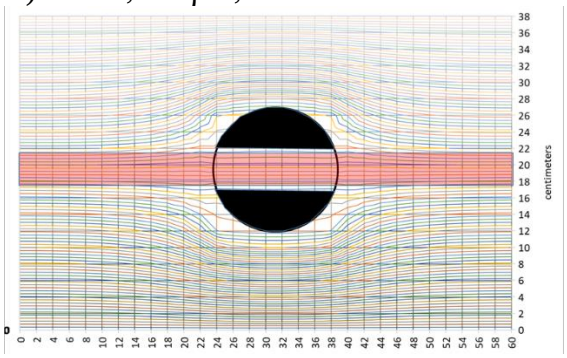

D) 2b = 10,000 µm; B = 2.65 cm

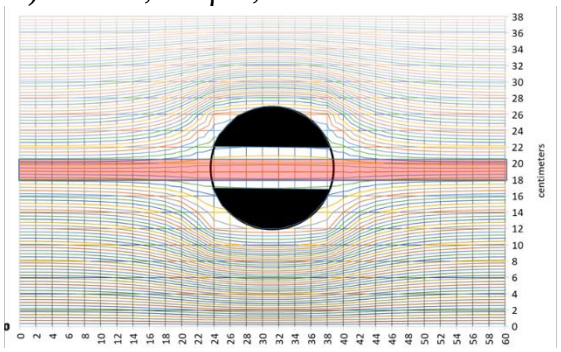

E) Relationship between 2b and B

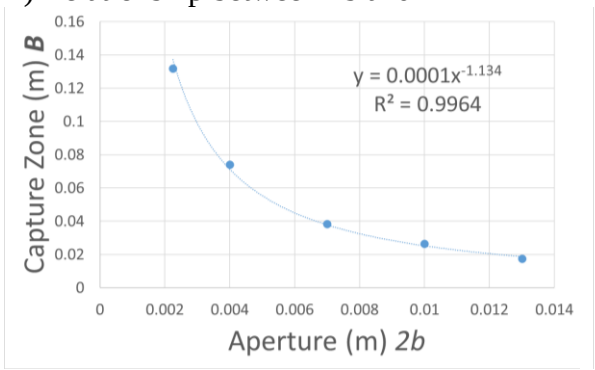

F) Relationship between 2b and cal. factor

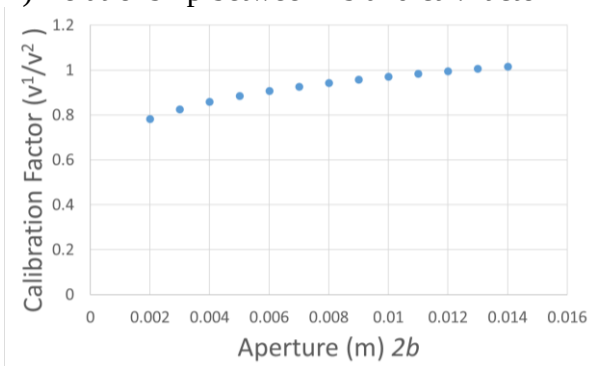

Figure 3.6: Simulations to estimate capture width as a function of fracture aperture, with a 15.8 cm diameter well and a grid size of 40 cm x 62 cm. The relationship is well described by the empirical equation $B_1 = .0001*x^{-1.134}$ for 2,250 µm < *2b* < 10,000 µm. Using this relationship and Equation 1, an empirical relationship between *q1/ q2* and fracture aperture was developed. Using this to plot a calibration line, and with estimates of fracture apertures available from the acoustic borehole televiewer in the uncased well, the flux in a fracture, *q1*, was determined from the flux measured in the probe, *q2*.

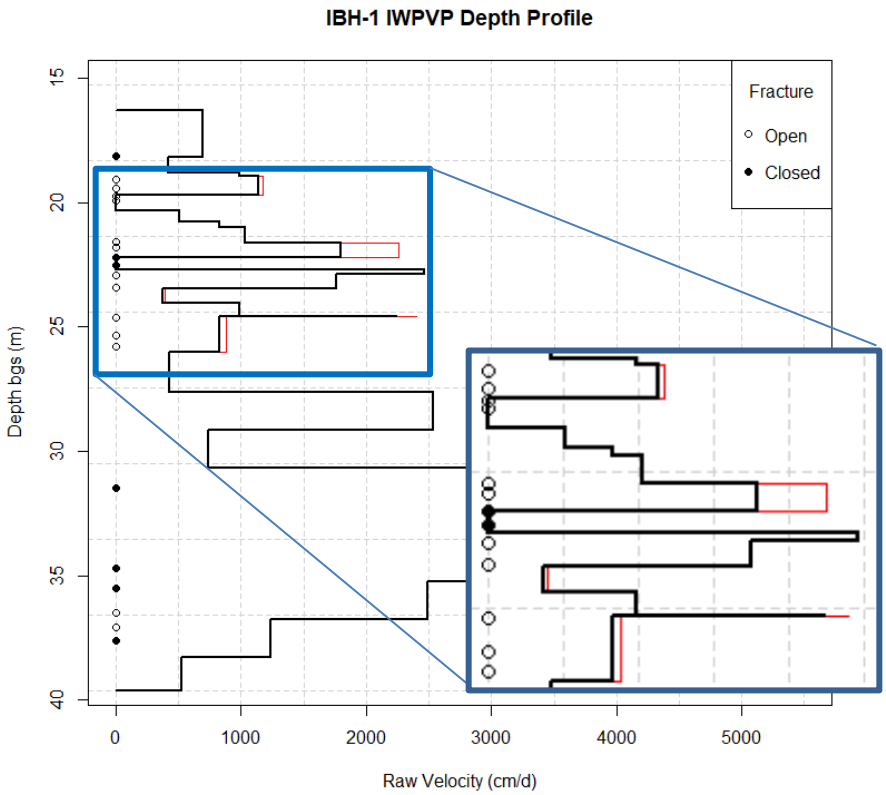

Figure 3.7: Depth profile of IWPVP flux measured in IBH-1 (red), with transformation of in-probe fluxes to aquifer fluxes highlighted (black), as well as open and closed fractures as identified by the acoustic borehole televiewer

3.6 – Discussion

3.6.1 – Relative Flux Profiles

A comparison of IWPVP flux profiles with those obtained from the PFM, ORP, and FLUTe technologies shows similar trends in flow as a function of depth: relatively high flow rates were observed in the depth range 21 m to 24 m, lower flow rates in the range 24 m to 26.5 m, a generally large relative flow between 32 m bgs and 36.5 m, and finally a rise in flow in the bottom few meters of the borehole at a depth of about 39 m (Figure 3.5). Some variations between the different methods are attributable in part to flow variations between the times the measurements were made. In addition, the differences in test locations (i.e., instrument positions

in the borehole and the fact that IW-01 and IBH-1 were located several meters apart) and sampling intervals (time and space) could have contributed to differences in the profiles. For example, the PFM results represent fluxes averaged over approximately 1 m of the borehole per data point, and flow was averaged over about three weeks, while the IWPVP sampled 2 cm of borehole per data point and each test lasted on the order of 10 to 15 minutes. In spite of these contrasting data collection methods, the general consistency of the flow profiles is encouraging. The consistency of the trends suggests that vertical short-circuiting in the borehole may have been secondary to horizontal flow in most of the boreholes. Furthermore, transience in the flow seems to have dissipated quickly, allowing steady state to be reestablished quickly enough that the major trends in relative flow rates with depth were preserved. This notion is supported by the short time over which flow directions at IBH-1 were altered by 180º following a rain event.

At IBH-1, a transmissivity depth profile was created by FLUTe liner deployment and was the only dataset available for direct comparison to the IWPVP results in that borehole. It is important to note that FLUTe liner estimates of transmissivity lose sensitivity with depth. Nevertheless, the resulting profiles can be useful in identifying relatively high transmissive zones. As before, good comparisons with the IWPVP data set exist. Locations of relatively fast flow indicated by the IWPVP generally coincided with high transmissivity zones indicated by the FLUTe liner (Figure 3.5). It is acknowledged that in spite of overall good agreement, the methods differed in some details. For example, the FLUTe liner suggested a conductive fracture at a depth of about 21.3 m that was not recorded in the IWPVP profiling. Similarly, the IWPVP detected flow at about 32 m depth that showed no corresponding feature in the FLUTe dataset. The reasons for these discrepancies may be related to the discrete nature of the IWPVP measurements, the different times that the data were collected (i.e., flow may have actually been

different on the days the measurements were made) or poorly understood patterns of vertical flow in the borehole.

Two depths in IBH-1 exhibited unusual characteristics that might have been associated with vertical flow in the borehole. At 20 m and 24 m depths, tests in which large tracer volumes (5 mL) were injected only produced weak signals. This might occur if tracer was cleared from the top or bottom of the central mixing chambers where the probe was designed to minimize signal detection to filter out signals from density driven flow. By plotting the cumulative flux over depth measured by the IWPVP, zones of possible vertical flow dominance (in the borehole) may be revealed. Shallow slopes on the resulting lines develop when of horizontal flow continuously adds to the flux total. A steep line slope results when no new flux adds to the total within a given depth range, i.e. a no-flow zone exists. Intermediate slopes with second derivatives near zero over a depth range between two fractures is suggestive of vertical flow in the borehole between the fractures. This arises because vertical flow causes near identical fluxes to be registered by the IWPVP over the affected range, producing a constant first derivative and a zero second derivative. A few locations suggest vertical flow, but the strongest indication according to cumulative flux and second derivative values occurs between 24 and 26 m bgs, also agreeing with BTC nature suggesting vertical flow dominance (Figure 3.8).

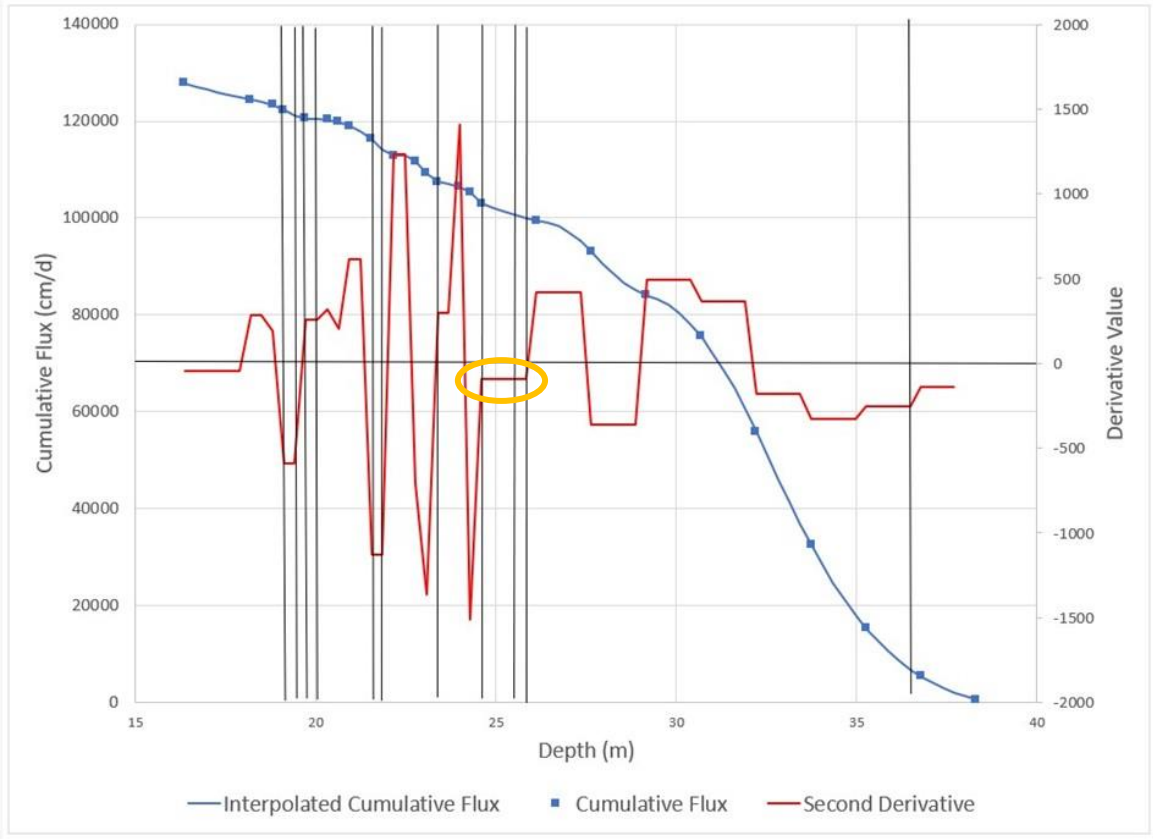

Figure 3.8: The cumulative flux and second derivative of cumulative values with depth measured by the IWPVP throughout the profiling of IBH-1. Grey vertical lines indicate fractures identified by ATV data. The circled depth interval suggests vertical flow dominance due to a second derivative close to zero between known fractures.

The ATV analysis of fracture apertures within the borehole revealed physical apertures for IBH-1 ranging from about 7,500 to 12,000 µm. Taking these into account, aquifer flux values from 400 cm/d to 2,200 cm/d were estimated for the respective fractures. These values are likely conservatively high for this site due in part to the ATV's detection limit of physical fractures (~2,500 µm), and the possibility that drilling artificially enhanced fracture apertures at the borehole wall. While only a few sampling depths could be used to estimate aquifer fluxes, the objective of demonstrating that the IWPVP can be used to measure flow in fractures was achieved.

3.6.2 – Flow Directions

The dominant flow directions in IW-01 (110º clockwise from N) compares reasonably well to the regional flow direction (~150º clockwise from N), based on historic water table measurements for the site. The difference is attributed to very different scales of the measurements (Figure 3.2, Figure 3.4). The occurrence of an apparent secondary flow direction (15° clockwise from N) in IW-01, which was 90° from the primary direction, raised the possibility that the secondary flow direction was an artifact imposed by the probe itself. However, during the testing period, the probe was rotated to different orientations in each borehole with no change to the depth-specific flow directions relative to true north, establishing that measured flow directions were not influenced by the probe channel orientations in any way. On this basis, the flow directions found by the IWPVP are considered representative of aquifer flow to within at least ±45º (a quadrant) (Figure 3.4). In only a few cases, flow directions different from the two dominant angles were measured. This suggests that the majority of fractures were hydraulically connected to the dominant ones, a finding that is not surprising since the rock at the site has been described as deeply weathered to the point of being locally unconsolidated (Dutcher *et al*., 1963).

The dominant flow directions at IBH-1, prior to a notable rain event, are also in accordance with expected regional flow direction. However, following the rain, the flow directions apparently and unexpectedly shifted between 180° and 280° (measured clockwise from true north). It is noted that flow measurements after the rainfall were made in the upper section of IBH-1, which was not sampled before the rain. Therefore, the flow direction shift could not be verified at common depths before and after the rain. Nevertheless, the relatively consistent flow directions in IW-01 through the borehole strongly suggests that recharge from the rain event rapidly affected flow in the shallow fractures intersecting IBH-1.

3.7 – Conclusion

The pilot fieldwork with the In-Well Point Velocity Probe in fractured media showed for the first time, that IWPVPs printed for different well diameters – 7.62 cm and 15 cm (3” and 6”) – functioned as designed at depths up to 38 m below ground surface. Design modifications that contributed to the success of the IWPVP in this application included a tracer injection point inside the probe repositioned from the top of the mixing chamber to its center, the addition of reinforcing plates to strengthen the probe body for deeper deployment, and the addition of a centralizer to the rod immediately above the probe to maintain proper positioning of the probe in the borehole.

In the cased well, IW-01, Darcy fluxes internal to the probe were found to vary between 300 – 3,500 cm/d. In the uncased well, IBH-1, Darcy internal fluxes ranged between 400 – 5,300 cm/d, a range not significantly different than IW-01. The flow through the boreholes appeared to be dominantly horizontal, though the IWPVP indicated the possibility of cross-fracture vertical flow at a depth range of 24 – 26 m bgs.

Trends in flow with depth determined by the IWPVP compared favorably with trends in fracture transmissivity based on FLUTe liner deployment, ORP measurements made with probes suspended in IW-01, and PFM devices. In general, the four methods revealed minimally variable fluxes to a depth of about 30 m, higher flows between 30 and 35 m, a decline in flow between 35 m and 38 m, and indications of increasing flow at greater depths. The various technologies produced profiles that differed in the finer details, but these differences are attributable to differences in the timings of the measurements (i.e., not simultaneous measurements), slight differences in the placements of the instrumentation in the boreholes, as well as the differences in spatial and temporal averaging associated with the instrument sizes and deployment times.

The IWPVP indicated a dominant flow direction that was within about 40° of the expected direction, based on a regional water table map. The probe also showed that the fractures were highly responsive to rainfall, which appeared to cause a pronounced change in the dominant direction of flow in at least the shallow fractures of one borehole (IBH-1).

The In-Well Point Velocity Probe was successful in measuring horizontal flow and flow directions in a field setting with fractured media at the Edwards Air Force Base. Additional work is recommended to refine methods for the conversion of fluxes inside the probe to fluxes within the fractures and to differentiate vertical from horizontal flow. Nevertheless, the probe was effective in identifying discretely transmissive zones that could be responsible for moving a significant contaminant mass. Moreover, the measurements were completed inexpensively and in near real-time.

3.8 – References

Alexander, M., Berg, S.J., Illman, W.A., 2011. Field Study of Hydrogeologic Characterization Methods in a Heterogeneous Aquifer. Ground Water 49, 365–382. https://doi.org/10.1111/j.1745-6584.2010.00729.x

Berkowitz, B., 2002. Characterizing flow and transport in fractured geological media : A review. Adv. Water Resour. 25, 861–884. https://doi.org/https://doi.org/10.1016/S0309-1708(02)00042-8

Butler, J.J., Dietrich, P., Wittig, V., Christy, T., 2007. Characterizing hydraulic conductivity with the direct-push permeameter. Ground Water 45, 409–419. https://doi.org/10.1111/j.1745-6584.2007.00300.x

Cherry, J.A., Parker, B.L., Keller, C., 2007. A new depth-discrete multilevel monitoring approach for fractured rock. Gr. Water Monit. Remediat. 27, 57–70. https://doi.org/10.1111/j.1745-6592.2007.00137.x

Devlin, J. F., & McElwee, C. D. (2007). Effects of measurement error on horizontal hydraulic gradient estimates. *Ground Water*, *45*(1), 62–73. https://doi.org/10.1111/j.1745-6584.2006.00249.x

Dutcher, L.C., Worts, G.F., 1963. Geology, hydrology, and water supply of Edwards Air Force Base, Kern, County, California.

Ghasemizadeh, R., Yu, X., Butscher, C., Hellweger, F., Padilla, I., Alshawabkeh, A., Cao, B.Y., 2015. Equivalent porous media (EPM) simulation of groundwater hydraulics and contaminant transport in Karst aquifers. PLoS One 10, 1–21. https://doi.org/10.1371/journal.pone.0138954

Hatfield, K., Annable, M., Cho, J., Rao, P.S.C., Klammler, H., 2004. A direct passive method for measuring water and contaminant fluxes in porous media. J. Contam. Hydrol. 75, 155–181. https://doi.org/10.1016/j.jconhyd.2004.06.005

Keller, C.E., Cherry, J.A., Parker, B.L., 2014. New method for continuous transmissivity profiling in fractured rock. Groundwater 52, 352–367. https://doi.org/10.1111/gwat.12064

Klammler, H., Hatfield, K., Newman, M.A., Cho, J., Annable, M.D., Parker, B.L., Cherry, J.A., Perminova, I., 2016. A new device for characterizing fracture networks and measuring groundwater and contaminant fluxes in fractured rock aquifers. Water Resour. Res. 52, 5400–5420. https://doi.org/10.1002/2015WR018389

Novakowski, K., Bickerton, G., Lapcevic, P., Voralek, J., Ross, N., 2006. Measurements of groundwater velocity in discrete rock fractures. J. Contam. Hydrol. 82, 44–60. https://doi.org/10.1016/j.jconhyd.2005.09.001

Novakowski, K.S., Evans, G. V., Lever, D.A., Raven, K.G., 1985. A Field Example of Measuring Hydrodynamic Dispersion in a Single Fracture. Water Resour. Res. 21, 1165–1174. https://doi.org/10.1029/WR021i008p01165

Osorno, T.C., Devlin, J.F., Firdous, R., 2018. An In-Well Point Velocity Probe for the rapid determination of groundwater velocity at the centimeter-scale. J. Hydrol. 557, 539–546. https://doi.org/10.1016/j.jhydrol.2017.12.033

Osorno, T.C., Devlin, J.F., Cormican, A., Heyer, B., Jones, M. 2020. Progress Update Report on IWPVP and PVP Data Analysis for Neodesha, KS, November 2019. Addendum to the Biosparge Pilot Test and Amendment Injection Workplan submitted by Sovereign Consulting Inc. to the Kansas Department of Health and Environment, May, 11 pp.

Parker, B.L., Cherry, J.A., Chapman, S.W., 2012. Discrete Fracture Network Approach for Studying Contamination in Fractured Rock. AQUA mundi 101–116. https://doi.org/10.4409/Am-052-12-0046

Pehme, P.E., Parker, B.L., Cherry, J.A., Greenhouse, J.P., 2010. Improved resolution of ambient flow through fractured rock with temperature logs. Ground Water 48, 191–205. https://doi.org/10.1111/j.1745-6584.2009.00639.x

Post, V.E.A., von Asmuth, J.R., 2013. Review: Hydraulic head measurements—new technologies, classic pitfalls. Hydrogeol. J. 21, 737–750. https://doi.org/10.1007/s10040-013-0969-0

Ricciardi, K.L., Pinder, G.F., Karatzas, G.P., 2009. Efficient Groundwater Remediation System Designs with Flow and Concentration Constraints Subject to Uncertainty. J. Water Resour. Plan. Manag. 135, 128–137. https://doi.org/10.1061/(asce)0733-9496(2009)135:2(128)

Schillig, P.C., 2012. VelProbePE: An automated spreadsheet program for interpreting point velocity probe breakthrough curves. Comput. Geosci. 39, 161–170. https://doi.org/10.1016/j.cageo.2011.06.007

Schillig, P.C. & Devlin, J.F., 2018. VELPROBE 3.1 BETA-d, www.people.ku.edu/~jfdevlin/software.html, accessed Sept. 15, 2020.

Shapiro, A.M., 2002. Cautions and Suggestions for Geochemical Sampling in Fractured Rock. Groundw. Monit. Remediat. 22, 151–164. https://doi.org/10.1111/j.1745-6592.2002.tb00764.x

van der Kamp, G. 1992. Evaluating the effects of fractures on solute transport through fractured clayey aquitards. Proceedings of the 1992 Conference of the International Association of Hydrogeologists, Canadian National Chapter, Hamilton, Ontario, May, 9 pp.

4.0 – Conclusions

This work has shown that the IWPVP can be used to characterize not only porous media, but also fractured rock. Laboratory and field investigations demonstrated the success of the tool, based on experiments using physical and numerical models. These efforts led to design changes to the IWPVP to increase performance in the fractured media. A field campaign provided evidence to support the probe's viability in characterizations and highlighted avenues for further research. Therefore, a major outcome of this work was the introduction and validation of a new tool for the characterization of fractured rock aquifers. More specific conclusions from the work follow in the sections below.

4.1 Fracture Flow Apparatus (FFA)

The physical fracture flow model established horizontal flow through a single fracture, simulating flow in a simple fractured rock aquifer. This was corroborated with numerical models. The FFA experiments led to the conclusion that the initial probe design was suitable for use in fractured media. Minor design adjustments were shown to improve the probe performance. These adjustments included 1) terminating the injection line in the center of the mixing chamber and 2) adding shoes at the top of the channels to permit deionized water to be used as the tracer without fear of interferences on the detectors from buoyancy-driven flow. The FFA experiments further established that bimodal BTCs can occur using the IWPVP. When they do, the first peak more reliably correlates to fracture flow rates than the second.

4.2 – Fracture IWPVP Calibration and Performance

The improved IWPVP design allowed accurate determinations of horizontal flux through the simulated fracture. Conducting tests at a variety of pumping speeds showed that the probe response was linear to fluxes up to about 80 m/d. It is further concluded that these calibration

factors are a function of the fracture aperture in the surrounding medium. On this basis, calibration factors could be determined for various aperture sizes. These experimentally determined factors compared well to calculated calibration factor values predicted from a flux balance equation that accounted for fracture aperture. From these calculations, it is further concluded that the calibration factors are correlated to the capture zone width of the well containing the probe. From a practical point of view, this latter dependency may not be too limiting since a capture zone width is only expected to vary between the diameter of the well and twice that diameter in most cases.

Under the idealized laboratory testing conditions of the FFA, the IWPVP was shown to accurately determine flow direction angles within about ± 20°. It is recognized that this level of performance may not be achievable in all settings (e.g. natural field conditions). However, the IWPVP is expected to reliably estimate flow directions to within at least ± 45°, simply on the basis of the probe's four-channel design. The initial laboratory work with the FFA and adapted probe design demonstrated the feasibility of the IWPVPs for characterizing flow in fractured rock.

4.3 – IWPVP Field Performance and Comparison

The field campaign carried out in conjunction with GSI Environmental at Edwards Air Force Base proved the adapted IWPVP to be viable in a field setting involving fractured rock. In addition to the modifications adopted following the FFA testing discussed previously, a borehole centralizer and reinforcing materials were added to the probe for the first time to permit deployment at depths up to 40 m below the ground surface. Additionally, custom probes were printed for the specific well sizes at the site – with diameters of 7.6 cm and 15 cm. From this it is concluded that the IWPVP can be deployed to depths of at least 40 meters.

Depth profiles consisting of in-probe fluxes were generated with the IWPVP for both uncased and cased wells. These relative flow profiles compared well to similar profiles developed by FLUTe liners, oxidation-reduction potential probes, and passive flux meters. The various technology profiles varied in some details, mostly likely due to variance in depths of deployment, times when measurements were made, and nature of the data being observed by each (i.e. differences in spatial and temporal averaging in data collected by instruments). Nevertheless, the general agreement leads to the conclusion that the IWPVP is a viable complementary tool to identify transmissive zones in the characterization of fracture media.

Dominant flow directions identified by the IWPVPs generally matched the expected flow direction identified by local water table maps. From this, it is concluded the flow direction capabilities demonstrated in the FFA are also present in field examples of fractured rock. The IWPVPs also indicated that flow direction within the transmissive zones was highly responsive to precipitation events (up to 180° directional change from the original). Rainfall during IWPVP testing caused the probes to return a wide variety of flow directions diverging from the expected flow direction with one direction dominant. Given the previous conclusion, this finding supports the additional conclusion that at the field site, flow direction in the shallower fractures responded very quickly to recharging groundwater with profound changes in flow direction. This phenomenon is a plausible occurrence with fractured media due to the high diffusivity possible in fractures. All in all, the IWPVP successfully measured horizontal flux and flow direction in fractured media in its typical inexpensive and timely manner.

4.4 – Estimation of Water Flux in Fractures

Acoustic borehole televiewer logs, collected by GSI Environmental, provided fracture locations and aperture sizes. Numerical modeling was used to estimate capture zone widths of

the uncased well as a function of well diameter and fracture aperture. A flux balance equation was used to estimate laboratory calibration factors based on the modeled flows inside and outside the probe. With this information, in-probe fluxes could be transformed to water fluxes in the fractures for wells of any size within the modeled range. With fracture apertures in the range of 7,500 to 12,000 μm overlapping IWPVP testing intervals, calibration factors ranged from 0.783 to 0.991. These estimates are considered maxima since the apertures visible at the borehole wall were generally large and possibly enhanced in the process of drilling the well. From this, it is concluded that the IWPVP can quantify flow in fractures within the range of 392 cm/d to 2,397 cm/d. This provides further validation of the IWPVP's ability to serve as a tool for characterizing sites underlain by fractured rock.

4.5 – Recommendations

Initial laboratory work was completed using a single horizontal fracture and a 5.08 cm diameter well. This is a highly idealized environment and not fully representative of the range of conditions that might be encountered in field applications. Future work should investigate the impact of multiple fractures within the IWPVP sampling interval on calibration factors, flux, and flow direction determinations. Similarly, a fracture flow apparatus with mock wells fabricated with larger diameters should be studied to confirm model predictions of the calibration factors.

Calibration factors estimated for the fractures at Edwards Air Force Base were first approximations based on the acoustic borehole televiewer data and a simple two-dimensional model. Additional site information and more detailed modeling techniques should be utilized to determine if more accurate calibration factors could be determined with additional effort and resources. Also, the flux in fractures could only be calculated at locations where the IWPVP sampling interval overlapped the location of a physical fracture seen in the televiewer log. Thus, further work should be conducted to extend the applicability of the method to all sampling

locations, both in cased and uncased wells. While the IWPVP is successful in measuring in-probe fluxes and thus relative transmissive and non-transmissive zones, identifying actual fracture fluxes would be a distinct advantage and requires additional characterization by new methods more sensitive to fracture size than the televiewer.

Working at depths of up 40 m below the ground surface introduced difficulties associated with tracer solution delivery due to large hydraulic gradients and cavitation of the fluid in the injection line. Therefore, alternative tracers that will not be impacted by this, e.g. heat-based tracers, should be developed and applied to the IWPVP. Additionally, the highly variable nature of fracture flow means there may be advantages to long-term deployments of the IWPVP. As a result, it could be advantageous to develop telemetric capabilities for the IWPVP so tests can be initiated remotely to allow data collection under at a variety of flow conditions and at times that site visits might be difficult to make.